Surface hydrolysis of sphingomyelin by the outer membrane protein Rv0888 supports replication of *Mycobacterium tuberculosis* in macrophages

Alexander Speer[1], **Jim Sun**[1], **Olga Danilchanka**[1,&], **Virginia Meikle**[1], **Jennifer L. Rowland**[1,#], **Kerstin Walter**[2,3], **Bradford R. Buck**[1], **Mikhail Pavlenok**[1], **Christoph Hölscher**[2,3,4], **Sabine Ehrt**[5], and **Michael Niederweis**[1,*]

[1]Department of Microbiology, University of Alabama at Birmingham, Birmingham, Alabama, United States of America

[2]Infection Immunology, Research Center Borstel, Borstel, Germany

[3]German Center for Infection Research

[4]Cluster of Excellence "Inflammation at Interfaces", Christian-Albrechts-University, Kiel, Germany

[5]Department of Microbiology and Immunology, Weill Cornell Medical College, New York, New York, United States of America

SUMMARY

Sphingomyelinases secreted by pathogenic bacteria play important roles in host-pathogen interactions ranging from interfering with phagocytosis and oxidative burst to iron acquisition. This study shows that the Mtb protein Rv0888 possesses potent sphingomyelinase activity cleaving sphingomyelin, a major lipid in eukaryotic cells, into ceramide and phosphocholine which are then utilized by Mtb as carbon, nitrogen and phosphorus sources, respectively. An Mtb *rv0888* deletion mutant did not grow on sphingomyelin as a sole carbon source anymore and replicated poorly in macrophages indicating that Mtb utilizes sphingomyelin during infection. Rv0888 is an unusual membrane protein with a surface-exposed C-terminal sphingomyelinase domain and a putative N-terminal channel domain that mediated glucose and phosphocholine uptake across the outer membrane in an *M. smegmatis* porin mutant. Hence, we propose to name Rv0888 as SpmT (sphingomyelinase of *M. tuberculosis*). Erythrocyte membranes contain up to 27% sphingomyelin. The finding that Rv0888 accounts for half of Mtb's hemolysis is consistent with its sphingomyelinase activity and the observation that Rv0888 levels are increased in the presence of erythrocytes and sphingomyelin by 5- and 100-fold, respectively. Thus, Rv0888 is a

*For correspondence: Phone: +1-205-975-4390, mnieder@uab.edu.
&Current address: Department of Microbiology and Immunobiology, Harvard Medical School, Boston, Massachusetts, United States of America
#Current address: Michael Smith Laboratories, University of British Columbia, Vancouver, British Columbia, Canada

novel outer membrane protein that enables Mtb to utilize sphingomyelin as a source of several essential nutrients during intracellular growth.

Keywords

lipid; heme; nutrient; uptake; cell surface; physiology

INTRODUCTION

Mycobacterium tuberculosis (Mtb), the etiologic agent of tuberculosis, co-evolved with humans and developed a complex metabolic network to effectively catabolize diverse nutrients available in its only known host (Ehrt & Rhee, 2013). These nutrients are simultaneously fed into downstream metabolic pathways, a phenomenon that is called co-catabolism. This metabolic plasticity enables Mtb to thrive in diverse niches during infection of humans (Ehrt & Rhee, 2013). After inhalation into the lung Mtb is phagocytosed by alveolar macrophages and dendritic cells. Mtb can proliferate in these cells, escape from the phagosome (van der Wel *et al.*, 2007, Simeone *et al.*, 2012) and migrate to local draining lymph nodes to disseminate and spread the infection (Russell *et al.*, 2009). Other, non-phagocytotic cells such as epithelial cells and adipocytes can also be infected by Mtb (Neyrolles *et al.*, 2006, Wolf *et al.*, 2007). The microenvironment in host cells encountered by Mtb is different as is the state of granulomas in the same host including caseating, fibrotic and cavitating lesions (Lin *et al.*, 2009, Barry *et al.*, 2009). However, a shared feature of the intracellular environments in which Mtb survives is the lack of nutrients commonly used by bacteria such as sugars, amino acids and trace metals, as the host immune system sequesters these solutes from invading bacteria. Thus, it is not surprising that Mtb relies on unusual nutrient sources such as fatty acids, lipids, and cholesterol at different stages of infection (Pandey & Sassetti, 2008, Puckett *et al.*, 2014, Watanabe *et al.*, 2011). However, except for cholesterol, *in vivo* nutrient sources of Mtb are unknown (Ehrt & Rhee, 2013, Niederweis *et al.*, 2010). Even less information is available on other nutrients providing Mtb *in vivo* with nitrogen, phosphorus, and iron (Niederweis et al., 2010).

Mycobacteria are protected by two membranes (Hoffmann *et al.*, 2008). While the inner membrane contains many specific transporter proteins (Niederweis, 2008), the outer membrane constitutes the major permeability barrier due to its unusual architecture and lipid composition (Brennan & Nikaido, 1995, Nikaido & Jarlier, 1991). Water-filled channel proteins, porins, enable diffusion of small, hydrophilic molecules across the outer membrane of Gram-negative bacteria (Nikaido, 2003). MspA is the main porin of *Mycobacterium smegmatis* (Stahl *et al.*, 2001) and mediates diffusion of small sugars, amino acids, and inorganic anions and cations across mycobacterial outer membrane (Stahl et al., 2001, Wolschendorf *et al.*, 2007, Song & Niederweis, 2012, Speer *et al.*, 2013a). Channel-forming proteins also exist in slow-growing mycobacteria such as Mtb (Kartmann *et al.*, 1999) and *M. bovis* BCG (Lichtinger *et al.*, 1999). Recently, the outer membrane channel protein CpnT of Mtb was discovered (Danilchanka *et al.*, 2014). A striking feature of CpnT is its two-domain organization that is different from classical porins, but resembles autotransporters of Gram-negative bacteria consisting of a channel-forming outer membrane domain and a

secreted or surface-exposed passenger domain (Leyton *et al.*, 2012). Likewise, the N-terminal domain of CpNT forms a channel that is embedded in the outer membrane and mediates uptake of glycerol, and the toxic C-terminal domain is secreted and induces a necrosis-like cell death of macrophages (Danilchanka et al., 2014). While such a combination of a nutrient transporter and a necrotizing toxin in a single protein is, to our knowledge, unprecedented, pathogenic bacteria utilize an array of toxins and secreted effector proteins to lyse host cells and mediate nutrient uptake during infection (Skaar, 2010). For example, bacterial pathogens secrete sphingomyelinases that hydrolyze sphingomyelin (SM), an abundant lipid in eukaryotic cells but not found in bacteria, to phosphocholine and ceramide (Oda *et al.*, 2010, Huseby *et al.*, 2007) and thereby lyse erythrocytes and release hemoglobin. Thereby, sphingomyelinases provide bacterial pathogens with iron and are important for bacterial virulence (McDonel, 1980, Huseby et al., 2007, Doll *et al.*, 2013, Oda *et al.*, 2012).

In this study, we identified the novel outer membrane protein Rv0888 as a sphingomyelinase, which is required for growth of Mtb on sphingomyelin and is also involved in uptake of the hydrolysis products. This function also explains the stimulating activity of sphingomyelin on growth of Mtb which was first described in 1948 (Dubos, 1948). While the N-terminus of Rv0888 is anchored in the outer membrane, the C-terminus has sphingomyelinase activity and is cell-surface exposed. Furthermore, Rv0888 lyses erythrocytes and constitutes the main hemolytic factor of Mtb. Thus, Rv0888 is a multi-functional protein utilized by Mtb for nutrient acquisition during infection.

RESULTS

Rv0888 facilitates glucose uptake and mediates a carbon source switch in *M. bovis* BCG

The channel protein CpNT mediates uptake of glycerol across the outer membrane of Mtb (Danilchanka et al., 2014). The uptake defect of the *M. bovis* BCG *cpnT* transposon mutant (*cpnT::Tn*) abolished growth in medium containing glycerol as the sole carbon source. Surprisingly, the *cpnT::Tn* mutant grew much better in medium containing glucose compared to wt *M. bovis* BCG (Fig. 1A). It is known that in some cases the lack of porins in Gram-negative bacteria and mycobacteria induces expression of silent porin genes (Stephan *et al.*, 2005, Blasband *et al.*, 1986, Fajardo *et al.*, 1998). Thus, we hypothesized that the switch of carbon source utilization to glucose in the *M. bovis* BCG *cpnT::Tn* mutant might have been caused by a silent outer membrane channel protein with a preference for glucose. To test this hypothesis, we profiled the transcriptome of wt *M. bovis* BCG and *cpnT::Tn* mutant grown in glycerol or glucose as sole carbon sources, respectively. The expression of 125 genes was induced by more than 1.5-fold in the *cpnT::Tn* mutant compared to wt (not shown). Only three of these genes are predicted to encode outer membrane proteins (Table S1) based on secondary structure analysis (Song *et al.*, 2008). We excluded proteins with homologs in *M. smegmatis*, because glucose uptake is mediated by Msp porins in this organism (Stephan et al., 2005) and focused on Rv0888 which is identical to Bcg0940 of *M. bovis* BCG. Indeed, a protein immunoblot showed five-fold increased Rv0888 protein levels in whole cell extracts of the *cpnT::Tn* mutant compared to wt *M. bovis* BCG (Fig. 1B). To examine whether Rv0888 is sufficient to mediate glucose utilization by *M. bovis* BCG, we

transformed wt *M. bovis* BCG with an *rv0888* expression plasmid (pML2118) and performed growth experiments in minimal medium. Constitutive expression of *rv0888* was sufficient to enable wt *M. bovis* BCG to grow in medium containing glucose as the sole carbon source in contrast to wt *M. bovis* BCG (Fig. 1A). Taken together, these results indicate that inactivation of *cpnT* increased expression of *rv0888* that enabled glucose utilization by the *cpnT::Tn* mutant of *M. bovis* BCG.

Rv0888 mediates glucose uptake across the outer membrane of *M. smegmatis* and is localized in the outer membrane of *M. tuberculosis*

The observation that the loss of the outer membrane channel protein CpnT increased expression levels of Rv0888 could be explained if both proteins have the same subcellular localization and similar functions. To examine whether Rv0888 has a porin-like activity, we exploited the pronounced permeability defects of the porin triple mutant of *M. smegmatis* ML16 lacking the porin genes *mspA, mspC* and *mspD* (Table S2) (Stephan et al., 2005, Speer *et al.*, 2013b). To this end the *rv0888* and *mspA* genes were expressed in ML16 (Fig. 1C). Indeed, the glucose uptake defect of *M. smegmatis* ML16 was complemented by expression of *mspA* and *rv0888* (Fig. 1D) indicating that Rv0888 facilitates glucose uptake across mycobacterial outer membranes. Next, we examined the subcellular localization of Rv0888. To this end, Mtb cells were lysed and the membrane fraction was separated from the water-soluble fraction as indicated by marker proteins. Western blot analysis revealed that Rv0888 is exclusively associated with the membrane fraction, but is not detected in culture filtrates (Fig. 2A). To distinguish between inner and outer membrane proteins, we used an approach that is based on surface detection of proteins in whole cells using antibodies and covalent modification with small molecules (Stahl et al., 2001, Danilchanka et al., 2014). Rv0888 was detected with a monoclonal anti-Rv0888 antibody in flow cytometry experiments using whole cells of Mtb overexpressing *rv0888* (Fig. 2B). This result indicated that Rv0888 is accessible on the cell surface of Mtb. Rv0888 was not detected in wt Mtb in these experiments due to low expression levels. Since overexpression of *rv0888* might lead to localization artifacts, we used an alternative assay based on covalent modification of surface proteins with the small molecule biotin (Voss *et al.*, 2014, Cao & Bazemore-Walker, 2014).

This assay is more sensitive due to sample concentration by affinity purification. We optimized the biotinylation assay to identify surface accessible proteins of low abundance in Mtb. To this end, cells of wt Mtb were treated with a membrane-impermeable biotin probe NHS-PEG$_{12}$-biotin that covalently binds to primary amino groups (Fig. S1A). As a control we used the membrane-permeable NHS-biotin (Fig. S1A), which biotinylates proteins with accessible lysine residues in all subcellular compartments. Mtb cells were lysed after biotinylation and water-soluble proteins were separated from membrane proteins by centrifugation at $100,000 \times g$ as shown by marker proteins (Fig. S1B). As expected the membrane permeable NHS-biotin probe biotinylated proteins in both fractions, while NHS-PEG$_{12}$-biotin probe mainly biotinylated membrane proteins (Fig. S1B). Biotinylated proteins were captured by NeutrAvidin beads and detected in immunoblot experiments. The protein fraction obtained from cells treated with NHS-biotin contained cytosolic proteins (IdeR, RNA polymerase) and inner membrane proteins (MmpS5, EccB5). By contrast, only

the surface-exposed protein LpqH (Wong *et al.*, 2011) was biotinylated with NHS-PEG$_{12}$-biotin (Fig. 2C), indicating that NHS-PEG$_{12}$-biotin does not penetrate the Mtb outer membrane under these conditions. Importantly, Rv0888 was biotinylated with NHS-PEG$_{12}$-biotin to the same extent as with NHS-biotin (Fig. 2C). These results are consistent with the surface detection of Rv0888 by flow cytometry (Fig. 2B). Thus, the surface accessibility experiments combined with the association of Rv0888 with the membrane fraction of Mtb indicate that Rv0888 is an outer membrane protein of Mtb. Outer membrane localization of Rv0888 is consistent with the functional complementation of glucose uptake by a porin mutant of *M. smegmatis* (Fig. 1D).

Bioinformatic analysis of Rv0888 predicts a membrane-spanning N-terminus and a C-terminal sphingomyelinase domain

Rv0888 is annotated as a protein of unknown function (Galagan *et al.*, 2010) and is not required for growth of Mtb *in vitro* (Zhang *et al.*, 2012) nor during infection (Sassetti & Rubin, 2003). Secondary structure analysis of the Rv0888 by the JPred algorithm (Cole *et al.*, 2008) indicated a putative domain rich in β-strands (residues 102 to 212) (Fig. S2A). Further analysis with Pred-TMBB revealed that five of eight predicted β-strands are amphiphilic, a feature characteristic of outer membrane but not of inner membrane proteins (Song et al., 2008). Furthermore, two hydrophobic α-helices were predicted in addition to the signal peptide near the N-terminus of the protein (Fig. S2A). Collectively, the bioinformatic analysis indicated secondary structural elements that are consistent with the localization of Rv0888 in the outer membrane.

The Rv0888 peptide sequence is similar only to proteins of unknown functions in the genus *Mycobacterium*. The C-terminus is predicted to belong to the large endonuclease/exonuclease/phosphatase family (Pfam family PF03372) (Finn *et al.*, 2014). 3D homology modeling (Kiefer *et al.*, 2009), revealed similarities to the *S. aureus* sphingomyelinase (Huseby et al., 2007) (Fig. S2B). Although the sequence similarity of Rv0888 and the sphingomyelinase of *S. aureus* is low, the sequence alignment showed that all residues conserved in other bacterial sphingomyelinases (Huseby et al., 2007) are present in Rv0888 (Fig. S2B). The highly conserved secondary structure in sphingomyelinases enabled us to predict the three-dimensional structure of the C-terminal domain of Rv0888 by homology modeling. The model of the Rv0888 sphingomyelinase domain is similar to the structure of the sphingomyelinase of *S. aureus* (Fig. S3). Based on this analysis we suggest a two-domain model for Rv0888 consisting of an N-terminal transmembrane domain and a C-terminal sphingomyelinase domain (Fig. 3A).

Expression of *rv0888* confers sphingomyelinase activity to *M. smegmatis*

To examine whether Rv0888 has sphingomyelinase activity, we expressed *rv0888* in *M. smegmatis*, whose genome does not encode a homolog of Rv0888. As a control we constructed the mutant Rv0888*, in which we mutated two conserved histidines in the catalytical center (H354N, H481N) of bacterial sphingomyelinases (Huseby et al., 2007). Importantly, expression of the *rv0888** mutant complemented the glucose uptake defect of *M. smegmatis* ML16 (Fig. 1D) and is detectable on the cell surface of Mtb in flow cytometry experiments (Fig. 2B) indicating that the mutations H354N and H481N did not interfere

with protein folding, export, and insertion of Rv0888 into the outer membrane. To directly measure the sphingomyelinase activity, cell lysates of *M. smegmatis* expressing *rv0888* and *rv0888** were incubated with purified sphingomyelin (SM) and the amount of undigested SM was determined by thin layer chromatography (TLC). SM was completely degraded by the whole cell lysate containing Rv0888, while the amount of SM was unchanged by cell lysates with Rv0888* or without Rv0888 (Fig. 3B). These results imply that Rv0888 is indeed a sphingomyelinase and that the histidines at positions 354 and/or 481 are required for the catalytic activity of Rv0888. It should be noted that the catalytically inactive Rv0888* mutant constitutes an important tool to distinguish between the nutrient uptake and sphingomyelinase activity of Rv0888.

Rv0888 is the only sphingomyelinase of *M. tuberculosis* detectable *in vitro*

To analyze the role of Rv0888 in Mtb, we constructed an *rv0888* deletion mutant by homologous recombination. The deletion of the *rv0888* gene was confirmed the by Southern and Western blot analysis (Fig. 3C, Fig. S4 A,C,D). Rv0888 was detected in a denaturing protein gel with an apparent electrophoretic mobility of a ~60 kDa protein, which is slightly above the predicted MW of the mature Rv0888 protein of 50 kDa. The Mtb   *rv0888* mutant was complemented by integration of a plasmid containing *rv0888* under control of the constitutive p_{wmyc} promoter into the mycobacteriophage L5 attachment site. Western blot analysis showed that the complemented strain ML923 overproduced Rv0888 compared to the wt under standard culture conditions by more than 500-fold (Figs. 3C, S5C). Whole cell lysates of wt Mtb showed three-fold higher sphingomyelinase activity compared to the   *rv0888* strain (ML1566) (Fig. S5). Importantly, complementation of the Mtb   *rv0888* mutant with an integrated *rv0888* expression cassette fully restored wt sphingomyelinase activity (Fig. S5). The apparent residual sphingomyelinase activity of the *rv0888* mutant could be due to other sphingomyelinases or result from other Mtb enzymes which interfere with the complex enzymatic sphingomyelinase assay. In order to investigate whether Rv0888 is the only sphingomyelinase in Mtb, we measured direct cleavage of radioactive SM, containing a ^{14}C-phosphocholine moiety. No conversion of SM to phosphocholine was detected in this highly sensitive assay after incubation with cell lysates of the Mtb *rv0888* mutant for 48 h (Fig. 3D), indicating that Rv0888 is the only sphingomyelinase of Mtb under these conditions. We noticed that the *rv0888* overexpressing strain ML923 had only a slightly higher enzymatic activity compared to wt Mtb despite much higher protein levels (Fig. S5). This could be an overexpression artifact leading to mislocalization of Rv0888 and accumulation of non-functional protein. Taken together, the sphingomyelinase activity of purified Rv0888 protein (Figs. 3E, 3F), the gain of sphingomyelinase activity by *M. smegmatis* after expression of *rv0888* (Fig. 3B) and the loss of sphingomyelinase activity in Mtb after deletion of *rv0888* (Fig. 3D) show that Rv0888 is a sphingomyelinase of Mtb.

Deletion and overexpression of *rv0888* do not change the susceptibility of *M. tuberculosis* and *M. smegmatis* for diverse antibiotics

The outer membrane is a major resistance determinant of mycobacteria against antibiotics (Brennan & Nikaido, 1995, Lambert, 2002). Compromising the outer membrane permeability barrier either by altering its lipid composition (Portevin *et al.*, 2004, Wang *et al.*, 2000) or by protein insertions (Stephan *et al.*, 2004, Danilchanka *et al.*, 2008b) makes

mycobacteria more susceptible to antibiotics. To examine whether the *rv0888* gene alters the outer membrane permeability nonspecifically, we determined the susceptibility of wt Mtb, the *rv0888* deletion mutant and the complemented strain which overexpresses *rv0888* (Fig. 3C) to a diverse set of antibiotics. None of the recombinant Mtb strains showed significantly altered drug susceptibility compared to wt Mtb (Table S3). Further, overexpression of *rv0888* in *M. smegmatis* did not change its drug susceptibility (Table S3). These results indicated that the function of the outer membrane as a permeability barrier is not impaired by the loss or overproduction of Rv0888. These results also show that the putative outer membrane channel of full-length Rv0888 does not increase the susceptibility of Mtb to the tested antibiotics in contrast to the porin MspA of *M. smegmatis* (Stephan et al., 2004, Mailaender *et al.*, 2004) or the autotransporter CpnT of Mtb (Danilchanka *et al.*, 2015).

The Rv0888 sphingomyelinase activity is detectable in the culture filtrate of *M. tuberculosis*

In numerous pathogenic bacteria sphingomyelinases are important virulence factors and are water-soluble proteins secreted into the extracellular space (Oda et al., 2012, Gonzalez-Zorn *et al.*, 1999). Although we did not detect Rv0888 in concentrated culture filtrates of Mtb by Western blot analysis (Fig. 2A), sphingomyelinase activity was detected by the highly sensitive ^{14}C-SM based assay (Fig. 3D). Importantly, no sphingomyelinase activity was detected in the culture filtrate obtained from the Mtb *rv0888* deletion strain ML1566, indicating that this minor SMase activity in the supernatant of Mtb may have resulted from membrane vesicles released from Mtb cells (Prados-Rosales *et al.*, 2011).

Purification and enzymatic characterization of Rv0888

To characterize the enzymatic properties of Rv0888, we targeted Rv0888 to the outer membrane of *E. coli*. To this end, the predicted signal sequence of Rv0888 was replaced with the signal sequence of the *E. coli* outer membrane protein OmpF and the recombinant gene was expressed in *E. coli*. Recombinant Rv0888 was extracted from the insoluble membrane fraction with the non-ionic detergent OPOE and purified by Ni-affinity chromatography. Using ^{14}C-SM as the substrate, the activity of Rv0888 was determined to be 1,480 U/mg of protein. Kinetics at various substrate concentrations using ^{14}C-SM (Fig. 3E, S6) revealed a Km of 671 μM which is similar to the substrate binding affinity of other sphingomyelinases (Table S4). The turnover number k_{cat} of Rv0888 was determined to be 1.8×10^3 s^{-1}.

To examine whether Rv0888 has sphingomyelinase activity when purified from mycobacteria, we expressed genes encoding Rv0888 and the catalytically inactive mutant Rv0888* C-terminally tagged with polyhistidine-HA in the porin mutant *M. smegmatis* ML375 (*mspA, mspC, mspD, groEL-5*′). The cells were first extracted with the detergent amidosulfobetaine-14 (ASB-14) to remove contaminating membrane proteins. Then, Rv0888 and Rv0888* proteins were extracted with Sarkosyl, purified by Ni-affinity chromatography and the detergent was exchanged by dialysis against 0.5% OPOE (Fig. S7). The activity of purified Rv0888 was 12 mU/mg, while the activity of Rv0888* was below the detection limit using the Amplex Red sphingomyelinase assay (He *et al.*, 2002) with purified *S. aureus* sphingomyelinase as an internal standard (Fig. 3F). These experiments

showed that functionally active Rv0888 was purified from *M. smegmatis*. However, the harsh detergents used for membrane extraction appeared to partially inactivate the Rv0888 protein.

The C-terminal sequence of Rv0888 is similar to neutral sphingomyelinases (Fig. S2B) (Clarke *et al.*, 2006). To confirm this classification, we tested the pH dependency of the Rv0888 sphingomyelinase activity using ^{14}C-SM as the substrate after adjusting the pH of cell lysates of *M. smegmatis* expressing *rv0888*. After two hours of incubation we observed a two-fold reduction in sphingomyelinase activity at a pH of 5.5 compared to the activity at pH 7.0. Only 3% of sphingomyelinase activity was detected at a pH of 4.5 (Fig. S8). Thus, Rv0888 is most active at neutral pH and is classified as a neutral sphingomyelinase.

Rv0888 is a major hemolytic factor of *M. tuberculosis*

Previous studies revealed that Mtb lyses erythrocytes upon cell-cell contact, but did not identify a molecular mechanism (King *et al.*, 1993). In this assay human erythrocytes and bacteria are co-sedimented and incubated for 24 h and hemoglobin release into the supernatant is quantified spectroscopically (Fig. 4A). Since the protein secretion system Esx-1 was previously described to contribute to the hemolytic activity of *Mycobacterium marinum* (Kennedy *et al.*, 2014), we analyzed an Esx-1 mutant of Mtb to validate this assay. Deletion of Esx-1 reduced the hemolytic activity of Mtb by 30% confirming the presumed role of Esx-1 in hemolysis also for Mtb (Fig. S9). Expression of *rv0888* in the *M. smegmatis* strain ML16 resulted in two-fold increase in hemoglobin release from red blood cells compared to the parent strain ML16 or the ML16 strain expressing *rv0888** encoding the catalytic mutant (Fig. 4A, B), indicating that Rv0888 mediates hemolysis in *M. smegmatis*. Next, we investigated whether Rv0888 contributes to the hemolytic activity of Mtb. Deletion of *rv0888* in Mtb reduced lysis of erythrocytes by two-fold compared to wt Mtb (Fig. 4C). These experiments show that Rv0888 is a major component of the hemolytic activity of Mtb. The Esx-1 system and other unknown factors account for approximately 30% and 20% of the hemolytic activity of Mtb, respectively. The cell-surface localization of the Rv0888 sphingomyelinase domain (Fig. 2) explains why cell contact is needed for Mtb to lyse erythrocytes (King et al., 1993). In our assay we observed equal hemolytic activity of wt Mtb and the *rv0888* mutant complemented with *rv0888*, despite the significant difference in Rv0888 levels in those strains when grown *in vitro* (Fig. 3C, lane 1&3). We therefore analyzed whether contact of Mtb with erythrocytes induces *rv0888* expression. Indeed, Rv0888 protein levels were increased by five-fold after contact with erythrocytes for 24 h (Fig. 4D).

M. tuberculosis utilizes Rv0888 to generate nutrients from sphingomyelin

Fatty acids are a carbon source preferred by Mtb *in vivo* (Schnappinger *et al.*, 2003). To examine whether SM or its cleavage products are utilized as carbon sources by Mtb, we measured growth of Mtb in minimal HdB medium with or without 0.75 mM sphingomyelin as the sole carbon source. Wt Mtb did not grow in HdB medium without SM demonstrating that this medium did not contain carbon sources sufficient to support growth. While the wt Mtb strain grew in the medium supplemented with SM, no growth of the *rv0888* deletion strain was observed under these conditions. This phenotype was complemented by

expression of *rv0888* but not by expression of the enzymatic mutant *rv0888** (Fig. 5A). These results showed that cleavage into phosphocholine and ceramide by Rv0888 is required for Mtb to utilize sphingomyelin as a carbon source *in vitro*. In order to investigate whether phosphocholine and/or ceramide are utilized by Mtb as carbon sources after cleavage of sphingomyelin we supplemented the medium with either compound and determined growth using the Alamar Blue assay. However, ceramide is a very hydrophobic lipid and precipitated in water despite the use of detergents or carrier proteins such as BSA. By contrast, medium supplemented with equimolar amounts of phosphocholine or sphingomyelin showed that sphingomyelin was utilized by wt Mtb and the complemented strain but not by the *rv0888* mutant or the *rv0888* mutant producing the non-catalytic Rv0888* mutant (Fig. 5B). Phosphocholine did not support growth of any tested strain when compared to medium with no carbon source, while medium supplemented with glucose and glycerol as carbon sources supported growth of all tested strains (Fig. 5B). We conclude from these experiments that ceramide is likely the cleavage product of sphingomyelin supporting growth of Mtb. The amount of Rv0888 protein in wt Mtb grown in standard 7H9 Middlebrook medium supplemented with OADC is very low and at the limit of detection by Western blot analysis. We tested whether *rv0888* expression is induced by sphingomyelin. Indeed, ~100-fold more Rv0888 protein were detected in wt Mtb grown in minimal medium with sphingomyelin as the sole carbon source to levels similar as observed in the *rv0888* overexpressing strain (ML923) (Fig. 3C). Induction of *rv0888* expression by sphingomyelin may also explain the increased Rv0888 levels by five-fold when Mtb was in contact with human erythrocytes (Fig. 4D) which contain up to 27% sphingomyelin of the total phospholipid content in their membrane (Bernheimer *et al.*, 1974).

Rv0888 enables *M. smegmatis* porin mutants to utilize phosphocholine as a phosphorus and nitrogen source

Based on the observation that Rv0888 enabled both *M. smegmatis* porin mutants and *M. bovis* BCG to take up glucose across the outer membrane (Fig. 1), we examined whether Rv0888 is also required for utilization of SM cleavage products generated by its sphingomyelinase activity. To this end, we exploited the low permeability of the *M. smegmatis* triple porin mutant ML16 for phosphate (Wolschendorf et al., 2007) which caused a strong growth defect on minimal agar plates containing only trace amounts of phosphorus (Fig. 6A). This permeability defect was fully complemented by expression of the porin gene *mspA* but not by *rv0888*, likely reflecting the different permeability properties of these channel proteins for phosphate. However, both genes fully restored growth of the *M. smegmatis* porin mutant ML16 on phosphocholine as the sole phosphorus source. A similar growth assay revealed that Rv0888 and MspA enable the *M. smegmatis* porin mutant to utilize phosphocholine also as the main nitrogen source (Fig. 6B), in contrast to the parent strain. These results indicate that Rv0888 mediates uptake of phosphocholine across mycobacterial outer membrane and that phosphocholine is utilized as both phosphorus and nitrogen source. These transport activities of Rv0888 do not require a functional sphingomyelinase domain as the catalytically inactive mutant Rv0888* fully substitutes for wt Rv0888 in these assays (Fig. 1D, Fig. 6B).

Rv0888 increases intracellular survival of *M. tuberculosis* and *M. smegmatis*

We performed macrophage infection experiments to examine whether Rv0888 plays a role in intracellular survival of Mtb. To this end, Mtb strains were grown in standard 7H9/OADC medium and differentiated THP-1 macrophages were infected. However, the *rv0888* deletion mutant replicated in macrophages to a similar extent as the parent strain (Fig. S10A). The very low R0888 protein levels in wt Mtb grown under standard conditions (Fig. 3C) may have masked a putative *in vivo* phenotype. Therefore, we first grew the Mtb strains in HdB medium supplemented with sphingomyelin. Glucose was also added to the medium to support growth of the *rv0888* deletion strain. As expected, the amount of Rv0888 protein in Mtb was significantly higher compared to Mtb grown in the standard 7H9/OADC medium (Fig. 3C). The Mtb strains conditioned in SM-containing medium were then used to infect THP-1 macrophages. Deletion of *rv0888* strongly impaired survival and/or replication of Mtb in infected THP-1 macrophages with eight-fold reduced bacterial numbers compared to wt Mtb (Fig. 7). This phenotype was partially complemented by expression of *rv0888* but not by *rv0888** encoding the non-catalytic mutant (Fig. 7) indicating that the cleavage of sphingomyelin by Rv0888 enhances replication of Mtb in macrophages. The importance of the catalytic domain for the function of Rv0888 was confirmed in similar infection experiments with *M. smegmatis. M. smegmatis* overexpressing *rv0888*, which showed enhanced intracellular survival compared to the strain expressing the functionally inactive mutant (Fig. S10B).

The level of ceramide increases on the cell surface of macrophages after infection with *M. tuberculosis*

Increased levels of ceramide, the cleavage product of sphingomyelin, in eukaryotic cell membranes have been linked to apoptotic cell death (Steinbrecher *et al.*, 2004). To assess whether the presence of Rv0888 during Mtb infections has an impact on host cell ceramide levels we infected THP-1 monocytes with Mtb and determined the amount of ceramide on the THP-1 cell surface by flow cytometry using a ceramide-specific antibody. The amount of surface-exposed ceramide increased 24 h after infection with Mtb in an MOI-dependent manner (Fig. S11A). However, loss of Rv0888 did not significantly change ceramide levels (Fig. S11B).

Rv0888 is not required for virulence of *M. tuberculosis* in mice

In order to investigate the role of Rv0888 in virulence of Mtb, we performed infection experiments with C57BL/6 mice. All Mtb strains contained the complex phthiocerol dimycocerosate (PDIM) lipids which are important for full virulence of Mtb in mice and are rapidly lost *in vitro* (Domenech & Reed, 2009) (Fig. S4B). The mice were infected by Mtb-containing aerosols or intravenously. Deletion of *rv0888* in Mtb did not alter the bacterial load in lung, liver and spleen over a period of 90 days (Fig. S12), indicating that Rv0888 does not play a role in virulence in the mouse model.

DISCUSSION

Rv0888 is a cell-surface sphingomyelinase of *M. tuberculosis*

Many pathogenic bacteria secrete sphingomyelinases that often are important virulence factors (Doll et al., 2013, Huseby et al., 2007). In this study, we identified Rv0888 as a sphingomyelinase of Mtb. Sphingomyelinase activity was observed earlier in Mtb, however, the corresponding Mtb enzyme(s) were either not identified (Vargas-Villarreal *et al.*, 2003) or not validated in Mtb mutants (Johansen *et al.*, 1996). The protein architecture of Rv0888 is unusual as the sphingomyelinase domain is attached to an outer membrane domain. Thus, Rv0888 is the first bacterial cell-surface sphingomyelinase in contrast to other bacterial sphingomyelinases which are secreted water-soluble proteins (Clarke et al., 2006).

M. tuberculosis employs Rv0888 to utilize sphingomyelin as a versatile nutrient source

In this study, we showed that Rv0888 enables Mtb to utilize sphingomyelin as a carbon, nitrogen, and phosphorus source in contrast to other lipids such as cholesterol which serves as a carbon source during infection (Griffin *et al.*, 2011), and requires the activity of a cluster comprising 82 genes (Van der Geize *et al.*, 2007). Sphingomyelin is an abundant lipid in the outer leaflet of the macrophage plasma membrane (Gaus *et al.*, 2005) which subsequently becomes the inner leaflet of the phagosome. Thus, sphingomyelin is readily available in the otherwise nutrient-poor environment of the phagosome enclosing Mtb after phagocytosis by macrophages. Our results suggest that Mtb uses the cell surface protein Rv0888 to utilize sphingomyelin as a nutrient *in vivo*. This hypothesis is not only supported by the findings that expression of *rv0888* is strongly induced by sphingomyelin *in vitro* (Fig. 3C) and after exposure of Mtb to low pH (Boshoff *et al.*, 2004), suggesting that phagocytosis might be an activating signal for *rv0888*. In contrast, expression of *rv0888* is repressed in non-replicating Mtb (Voskuil *et al.*, 2004) which is consistent with the reduced need for nutrient acquisition in periods of low metabolic activity. The utilization of sphingomyelin is also consistent with numerous indirect observations indicating the importance of lipids as a nutrient source for Mtb *in vivo* (Schnappinger et al., 2003, Russell *et al.*, 2010). It is conceivable that Mtb has the potential to use other lipids available in the phagosomal membrane in a similar manner. The most prevalent lipids in the macrophage plasma membrane are phospholipids (Gaus et al., 2005). Not surprisingly, Mtb encodes many phospholipases (Raynaud *et al.*, 2002, Xu *et al.*, 2010, Parker *et al.*, 2009). This versatility of Mtb in using lipids as nutrients is likely the reason why gene deletions eliminating the ability of Mtb to use a single lipid do not affect its survival *in vivo*. Taken together, our results indicate that Mtb utilizes sphingomyelin as a versatile nutrient possibly providing nitrogen and phosphorus in addition to carbon during infection.

Rv0888 is a novel outer membrane protein of *M. tuberculosis*

In this study, we showed that Rv0888 complements the uptake phenotypes of porin mutants of *M. smegmatis* (Fig. 1). These characteristics suggest that Rv0888 is a novel outer membrane protein of Mtb. Bioinformatic analysis indicated amphiphilic β-strands in the N-terminus of Rv0888, a feature characteristic of outer membrane β-barrel proteins (Song et al., 2008). However, the exact boundaries of the integral membrane domain of Rv0888 are unknown. To our knowledge Rv0888 is the first report of a protein with a sphingomyelinase

domain in conjunction with an outer membrane channel. An advantage of this combination could be that uptake of sphingomyelin cleavage products might be more efficient. It is striking that CpnT, the only other outer membrane protein of Mtb with a proven role in nutrient uptake, is also composed of two domains in an arrangement which is reminiscent of autotransporters (Danilchanka et al., 2014). Interestingly, in pathogenic mycobacteria the N-terminal channel domain of CpnT is conserved and is connected to highly divergent C-terminal domains (Danilchanka et al., 2014, Boritsch *et al.*, 2014). By contrast, the entire Rv0888 protein is highly conserved in mycobacteria indicating a functional connection between the C-terminal sphingomyelinase domain and the N-terminal channel domain.

Over-expression of *rv0888* after loss of the outer membrane channel protein CpnT (Danilchanka et al., 2014) was sufficient to enable *M. bovis* BCG to utilize glucose as the sole carbon source (Fig. 1B). These results indicate that the inability of *M. bovis* BCG to utilize glucose is caused by the lack of uptake which is overcome by a switch of outer membrane proteins. This is in contrast to previous reports suggesting an altered catabolism of *M. bovis* BCG to explain this phenotype (Keating *et al.*, 2005, Lofthouse *et al.*, 2013). Infection studies revealed that a double mutant lacking genes encoding the glucokinases PPGK and GLKA did not persist in lungs of infected mice demonstrating that glucose plays a role as carbon and/or energy source during chronic infections of mice (Marrero *et al.*, 2013). However, the Mtb rv0888 deletion mutant still grew on glucose as the sole carbon source, suggesting that Mtb can use other outer membrane proteins for glucose uptake. Our growth experiments with *M. smegmatis* porin mutants indicated that Rv0888 also mediates the outer membrane passage of phosphocholine (Fig. 6). Identification of the pore-forming domain of Rv0888 in combination with uptake experiments and biochemical and structural characterization is necessary to understand the transport function of Rv0888.

Rv0888 is a major hemolytic factor of *M. tuberculosis*

Mtb requires iron as an essential trace element similar to almost all bacteria (Skaar, 2010). Acquisition of iron is likely important for virulence of Mtb, although this has not been formally proven yet (Niederweis *et al.*, 2014). Previous studies revealed that Mtb lyses erythrocytes (King et al., 1993) and can utilize heme as a sole iron source (Jones & Niederweis, 2011). In this study we showed that not only the presence of sphingomyelin in culture medium (Fig. 3C), but also contact of Mtb with cells containing membranes rich in sphingomyelin such as erythrocytes (Fig. 4D) strongly increase Rv0888 expression levels. This is consistent with increased lysis of erythrocytes by Mtb strains that have sphingomyelinase activity (Fig. 4C). ESAT-6 forms pores in lipid membranes and was shown to contribute to hemolysis by *Mycobacterium marinum* (Smith *et al.*, 2008). In this study, we show that Rv0888 and the ESX-1 protein secretion system are the main hemolytic factors contributing approximately 50% and 30%, respectively, to the hemolytic activity of Mtb (Fig. S9). Heme from erythrocytes is not the only iron source for Mtb. Mtb secretes the siderophores mycobactin and carboxymycobactin to bind and take up iron with high affinity (Ratledge, 2004). Combinations of mutations in these iron acquisition pathways will be needed to assess the contribution of Rv0888 to iron acquisition by Mtb (Neyrolles *et al.*, 2015).

The sphingomyelinase Rv0888 enhances intracellular replication of *M. tuberculosis* in human macrophages

Infection experiments showed that the *rv0888* mutant of Mtb is attenuated in human macrophages compared to wt Mtb (Fig. 7). The enhanced intracellular replication of *rv0888* expressing Mtb requires a functional SMase domain and may be explained by the Rv0888-mediated availability of nutrients from sphingomyelin in the otherwise nutrient-starved phagosomes of macrophages (Russell, 2011, Rohde *et al.*, 2007). Interestingly, expression of a non-catalytic Rv0888 mutant was detrimental even for the already impaired *rv0888* mutant of Mtb. This observation is consistent with previous findings that the presence of proteins with channel activity in the outer membrane makes Mtb more susceptible to toxic solutes such as nitric oxide produced my macrophages to control growth of Mtb (Fabrino *et al.*, 2009, Danilchanka et al., 2015). However, mouse infection experiments did not reveal a virulence defect of the Mtb *rv0888* mutant. This may be due to the much lower sphingomyelinase content in cell membranes of mice. For example, erythrocytes of guinea pigs and mice are virtually resistant towards sphingomyelinases as their SM levels are only approximately 10% of the total phospholipid content. By contrast, sheep (51% SM) and human erythrocytes (~20–27% SM) have high and intermediate sensitivity to lysis by sphingomyelinases (Ingraham *et al.*, 1981, Bernheimer et al., 1974). Thus, Rv0888 may play a more important role during human infection than what can be assessed using current mouse models.

Conclusions

To our knowledge, Rv0888 is the first protein with coupled sphingomyelinase and channel domains. In this study we show that Rv0888 enables Mtb to utilize sphingomyelin as a nutrient source for carbon, nitrogen and phosphorous (Fig. 8). To use an abundant lipid in the phagosomal membrane to obtain nitrogen and phosphorus in addition to the established function of lipids as a carbon and energy source appears to be an elegant survival mechanism of Mtb in nutrient-starved phagosomes. Similar mechanisms may also apply to the acquisition of other essential elements such as sulfur from host cell lipids by Mtb. Based on these findings, we propose to name Rv0888 as SpmT (sphingomyelinase of *M. tuberculosis*), which constitutes the founding member of a novel class of outer membrane proteins. The functional characterization of SpmT also indicates that Mtb utilizes autotransporters not only for protein secretion and/or cell-surface presentation, but also for nutrient uptake. This novel mechanism uses the resources invested in protein synthesis most efficiently and simultaneously improves the efficiency of nutrient uptake by combining the substrate generation and transport in the same protein.

Materials and Methods

Subcellular fractionation of soluble, membrane associated and secreted proteins

A wt Mtb mc^{2}6206 culture was grown in Sauton's medium with 0.02% tyloxapol until OD_{600} reached 3.0. Afterwards, the cells were harvested, washed with detergent free Sauton's medium and used to inoculate 150 mL of Sauton's medium at an OD_{600} of 0.1. At the same time a culture with tyloxapol was inoculated in order to track the optical density. After the OD_{600} reached 1.8 the detergent free culture was harvested by centrifugation and

the obtained cell pellet was washed twice in PBS (140 mM NaCl, 2 mM KCl, 10 mM Na_2HPO_4/NaH_2PO_4, pH 7.4). The culture supernatant was filtered (Millipore, Stericup Express Plus, pore size 0.22 μm) and concentrated by ultrafiltration (Amicon Ultra, Ultracel-3K, cut off size 3 kDa) to 300 μL. The cell pellet was resuspended in PBS (0.25 g/mL) containing 1 mM phenylmethanesulfonylfluoride (PMSF) and lysed by sonication (450 cycles, 1 s on, 1 s off, output 12 W) (MISONIX sonicator 3000). The crude lysate was incubated with 50 U Benzonase (Novagen) and 1 mg/ml lysozyme at 37°C for 1 h while shaking at 200 rpm. Cell debris and unbroken cells were removed by centrifugation (3,000 × g, 10 min, 4°C) and the supernatant was diluted 5-fold in PBS (WCL). To separate soluble from insoluble proteins the lysate was centrifuged at high speed (135,000 × g, 1 h, 4°C). The soluble protein containing supernatant (SN1) was removed and the pellet (P1) was resuspended in PBS to the original volume. Both fractions were centrifuged a second time (135,000 × g, 1 h, 4°C). The supernatant of SN1 was transferred into a new tube and contains soluble proteins (SN2). The insoluble proteins containing pellet of P1 was separated from the supernatant and resuspended in PBS to the original volume (P2). The fractions were analyzed by SDS-PAGE and Western blot analysis.

Surface detection of proteins in *M. tuberculosis* by flow cytometry

The parent strain Mtb ML1528 (H37Rv L5::pCV125), the *rv0888* mutant ML1566 and the complemented mutants strains overexpressing either *rv0888* (ML923) or *rv0888** (ML925) were grown to mid-log phase and were fixed with 4% paraformaldehyde for 30 min at room temperature (see table S7 for strains used in this study). The cells were washed twice with PBS/tyloxapol (0.02%) before incubation with monoclonal anti-Rv0888 antibody (10E2.7) at a dilution of 1:1 in PBS/tyloxapol (0.02%) for 30 min at room temperature to stain the bacterial surface. Following three washes, bacteria were stained with anti-mouse FITC-antibodies at a dilution of 1:500 for 30 min. Bacteria were washed three times and analyzed by flow cytometry. Surface accessible Rv0888 was quantified by measuring fluorescence and displayed as histograms.

Surface biotinylation of proteins in whole cells of *M. tuberculosis*

Mtb mc²6206 was grown in Middlebrook 7H9/OADC/tyloxapol/leucine/pantothenate/casamino acids after adjustment of the pH to 7.4. A dense culture (5 mL) was filtered (pore size 5 μm) to remove clumps and was then used to inoculate 250 mL at an OD_{600} of 0.05. The cells were grown at 37°C in bottles on a bottle roller incubator to an OD_{600} of 0.8. Cells were harvested (2,500 × g, 4°C, 10 min) and washed three times by soft resuspension in ice cold PBS/tyloxapol (0.01%) and resuspended in PBS/tyloxapol (6 ml PBS/1 g wet cells pellet). Into 500 μL of cell suspension 10 μL of 25 μM NHS-PEG$_{12}$-Biotin (EZ-Link NHS-PEG12-Biotin, Pierce), 25 μM NHS-Biotin (EZ-Link Sulfo-NHS-Biotin, Pierce) or DMSO were added. The samples were incubated on a rotary shaker at 4°C for 20 min. The reaction was quenched by washing three times with 5 mL stopping buffer (50 mM Tris-HCl, pH 8.0, 100 mM glycine, 0.01% tyloxapol) for 5 min at 4°C on a rotary shaker. The biotinylated cells were resuspended in 500 μL of lysis buffer (PBS, 1 mM PMSF, 300 mM Tris-HCl, pH 8.0, 20% (v/v) protease inhibitor (cOmplete/Roche)). The cells were lysed on ice by sonication (300 cycles, 1 s on, 1 s off, output 15 W). After addition of 5 μL of 100 mM PMSF, 50 μL of lysozyme (10 mg/mL) and 50 U Benzonase (Novagen) the lysates were

incubated for 30 min at 37°C. To extract membrane proteins SDS was added to a final concentration of 1% (w/v) and extraction was performed at 80°C for 20 min. Insoluble material was removed by centrifugation (16,000 × g, 5 min, room temperature) and the extracted proteins were transferred into new vials. The protein concentration was determined by BCA assay (Thermo). 150 μL of NeutrAvidin UltraLink resin (Thermo) was washed two times for 5 min with 500 μL of PBS containing 1% (w/v) SDS and 0.25 mg/mL BSA at room temperature. 5 mg of extracted protein was added to the resin and the biotinylated proteins were allowed to bind for 1 h at room temperature on a rotary shaker. Afterwards the resin was washed two times with 1 mL of wash buffers A-D (after addition of each wash buffer the resin was incubated on a rotary shaker for 5 min). A: 8 M Urea, 0.2 M NaCl, 2% (w/v) SDS, 0.1 M Tris-HCl (pH 8.0), B: 8 M Urea, 1.2 M NaCl, 1% (w/v) SDS, 0.1 M Tris-HCl (pH 8.0), 10% (v/v) ethanol, 10% (v/v) isopropanol, C: 8 M Urea, 0.2 M NaCl, 1% (w/v) SDS, 0.1 M Tris-HCl (pH 8.0), 10% (v/v) ethanol, 10% (v/v) isopropanol, D: 8 M Urea, 1% (w/v) SDS, 0.1 M Tris-HCl (pH 8.0). The biotinylated proteins were removed from the resin by resuspending beads in 150 μL of four-fold protein loading buffer (250 mM Tris-base, 8% (w/v) SDS, 40% (v/v) glycerol, 0.4% (w/v) Bromophenol Blue) and heating to 95°C for 15 min. The beads were removed by centrifugation and the eluted proteins were analyzed by Western blotting.

Purification of Rv0888 from *M. smegmatis*

rv0888-*HA-His* (pML2100) or the enzymatic mutant *rv0888**-*HA-His* (pML3109) were expressed in *M. smegmatis* strain ML375 under the control of the nitrile inducible expression system (Pandey *et al.*, 2009). At an OD_{600} of 0.6 the cells were induced by addition of 5 μM Isovaleronitrile for 48 h (200 rpm, 37°C). The cells were harvested by centrifugation (5,000 × g, 15 min, 4°C) and washed with PBS/tyloxapol (0.02%). Afterwards a cell pellet corresponding to 250 mL of culture was resuspended in 15 mL of lysis buffer (50 mM Tris-HCl, pH 7.4, 300 mM NaCl, 1 mg/mL lysozyme, 50 U Benzonase (Novagen), 1 mM PMSF) and lysed by sonication (300 cycles, 1 s on, 1 s off, output 21 W) (MISONIX sonicator 3000). The lysates were incubated for 1 h at 37°C to allow DNase and lysozyme to digest. The soluble proteins were removed from the Rv0888 containing membrane fraction after centrifugation (140,000 × g, 1 h, 4°C) and the pellet was extracted with 1% (w/v) ASB-14 in binding buffer (50 mM Tris-HCl, pH 7.4, 300 mM NaCl, 10 mM Imidazole, 1 mM PMSF,) for 2 h at 37°C. Proteins that were solubilized by ASB-14 were removed after centrifugation (140,000 × g, 1 h, 20°C) and the pellet was extracted with 1% (w/v) Sarkosyl in binding buffer for 2 h at 37°C. Afterwards, insoluble cell parts were removed by centrifugation and the extract was diluted five-fold in binding buffer in order to dilute the Sarkosyl concentration to 0.2%. Diluted protein extracts corresponding to 125 mL of culture were incubated with 4 mL of 50% Ni-NTA Agarose beads (HisPur Ni-NTA Resin, Thermo) on a rotary shaker at 4°C overnight. The beads were transferred into a gravity flow column and washed with 100 CV of binding buffer with 0.2% (w/v) Sarkosyl and 50 CV of washing buffer (50 mM Tris-HCl, 300 mM NaCl, 20 mM Imidazole, 1 mM PMSF, pH 7.4, 0.2% (w/v) Sarkosyl). Afterwards the protein was eluted with elution buffer (50 mM Tris-HCl, pH 7.4, 300 mM NaCl, 250 mM Imidazole, 1 mM PMSF, 0.2% (w/v) Sarkosyl) into 0.5 CV fractions. The fractions containing the majority of Rv0888 were pooled and 0.5% (v/v) OPOE was added. Sarkosyl was removed by dialysis against 50 mM

Tris-HCl, 300 mM NaCl, pH 7.4 using dialysis tubes (12–14 kDa, D-Tube, Novagen) for 48 h.

Hemolysis of *M. smegmatis* and Mtb

M. smegmatis strain ML16 carrying the plasmids pMS2, pML2118 or pML3108 were grown in Middlebrook 7H9/tyloxapol to mid-logarithmic phase. Afterwards the cells were harvested and washed in reaction buffer (50 mM Tris-HCl, pH 7.2, 10 mM $MgCl_2$, 0.66 mM $CaCl_2$, 100 mM NaCl) and the OD_{600} was adjusted to 1.0. Then 300 μL of the cell suspension were transferred into a reaction tube and the buffer was removed by centrifugation. Human blood cells (obtained from Hematology lab, UAB) in heparin (200 U/mL) were diluted in reaction buffer and 1×10^6 cells were used to resuspend the *M. smegmatis* cell pellets. The blood and *M. smegmatis* cells were co-pelleted ($8,000 \times g$, 15 sec, 20°C) and incubated for 24 h at 37°C. Afterwards, the cells were carefully resuspended and again pelleted ($8,000 \times g$, 15 sec, 20°C) to remove intact cells and cell debris. The supernatant was removed and the absorbance at 540 nm was determined.

The Mtb hemolysis experiments were performed as previously described (King et al., 1993). Briefly, *Mtb* strains were grown in Middlebrook 7H9/OADC/tyloxapol/kan to an OD_{600} of 3.0. The cells were harvested ($3250 \times g$, 10 min, 20°C) and washed with reaction buffer (50 mM Tris-HCl, pH 7.2, $MgCl_2$ 10 mM, $CaCl_2$ 0.66 mM) supplemented with 1% (w/v) BSA and 142 mM NaCl. After the OD_{600} was adjusted among the strains 1×10^{10} cells (OD_{600} 1.0 = 3×10^8 bacteria) were transferred into a new tube and the buffer was removed by centrifugation. The Mtb cell pellet was resuspended in 1 mL reaction buffer containing 2×10^7 red blood cells/mL to yield an MOI of 500. Afterwards, the cells were co-pelleted ($8,000 \times g$, 1 min, 20°C) and incubated for 24 h at 37°C. The cells were resuspended and pelleted ($8,000 \times g$, 1 min, 20°C) before the supernatants were removed to determine the absorbance at 540 nm. The reaction buffer in experiments with Mtb strains mc²6230 (ΔleuCD, ΔpanCD) and mc²6203 (ΔRD1, ΔpanCD) was additionally supplemented with pantothenic acid (12 μg/mL) and leucin (25 μg/mL).

THP-1 macrophages infection experiments

THP-1 macrophages were seeded on 96-well plates (1×10^5 cells/well) and differentiated overnight with 100 ng/mL 2-phorbol 13-myristate acetate (PMA). Macrophages were washed and replenished with culture media without antibiotics 2 h prior to infection with Mtb or M. smegmatis strain. Bacteria growing in mid-log phase were normalized by optical density (OD_{600} 1.0 = 3×10^8 bacteria), washed and opsonized in infection media containing 2% normal human serum (Millipore) for 15 min at 37°C. Macrophages were then infected with Mtb strains ML1528 (H37Rv L5::pCV125), ML1566 (Δrv0888), ML923 (Δrv0888 + rv0888), or ML925 (Δrv0888+rv0888*) or *M. smegmatis* SMR5 (wt), SMR5 pML2118 (wt +rv0888), SMR5 pML3108 (wt+rv0888*) at a multiplicity of infection (MOI) of 1 or 100, respectively. Macrophage monolayers were then washed 3 times with PBS 3 h post-infection and replenished with culture media containing 50 μg/mL gentamycin. After 1 h the wells designated for 4 h (*M. smegmatis*) or day 0 (Mtb) were washed twice with PBS before the macrophages were lysed by addition of PBS/SDS 0.025% (w/v). Mtb containing wells were washed after 24h to remove gentamycin and medium containing no antibiotics was added.

On the indicated time point attached (viable) and detached (non-viable) macrophages were collected by centrifugation ($5,000 \times g$, 5 min) to ensure all Mtb cells were accounted for. Serial dilutions of recovered bacteria were then plated on solid 7H10 media supplemented with 10% OADC and kanamycin. CFU counts were performed after 2 weeks of incubation at 37°C.

Sphingomyelinase activity assays by thin layer chromatography

Samples were prepared for analysis as described in the supplementary information. 20 μg purified sphingomyelin (from chicken egg yolk, Sigma) was dissolved in ethanol (100 mg/mL) and was added into tubes for each reaction. The ethanol was allowed to evaporate, the remaining SM was resuspended in 10 μL sphingomyelinase reaction buffer (50 mM Tris-HCl pH 7.4, 10 mM $MgCl_2$, 0.66 mM $CaCl_2$, 1% (v/v) Triton-X100) and 10 μL of the test sample were added. At each time point 1 μL of the reaction mixture was transferred onto a TLC plate (Silica gel on TLC AL foils, Fulka). The TLC was resolved with chloroform/methanol/water (65:25:4). Phospholipids were visualized by spraying Dittmer-Lester reagent (Sigma) on the TLC. To achieve a more sensitive detection of sphingomyelinase activity ^{14}C-sphingomyelin (ARC, choline methyl-[^{14}C]) was used as a substrate as indicated. Radioactivity was visualized using a phosphor screen (GE-Healthcare) and a phosphor imager (Amersham, Storm 820).

Enzyme coupled assay to measure sphingomyelinase activity

A detailed description how samples were prepared prior to analysis is provided in the supplementary information. The Amplex Red Sphingomyelinase Assay (Molecular Probes) provides a sensitive, rapid, and simple fluorometric method for detecting very low concentrations of sphingomyelinase and was used according to the manufacturer's recommendations. Purified sphingomyelinase of *S. aureus* with a known activity (one unit hydrolyzes 1.0 μmol of sphingomyelin per min at pH 7.4 at 37°C) was used as a standard.

Kinetic studies of the sphingomyelinase activity of Rv0888

To determine the Michaelis-Menten constant of Rv0888$_{HAHis}$, the enzyme was purified from *E. coli*. ^{14}C-sphingomyelin (SM) was diluted in ethanol to 56 mM and non-labeled SM was added to yield a final concentration of total SM of 56 mM, 112 mM, 225 mM, 450 mM and 900 mM. The recombinant Rv0888 protein was added at an concentration of 14.6 pM and after 1 min, 2.5 min and 5 min samples were taken and diluted 1:1 in ethanol in order to stop the reaction. The samples were resolved by TLC together with a standard of ^{14}C-SM (0.18 μM, 0.35 μM, 1.8 μM, 3.5 μM, 18 μM, 35 μM). The TLCs were exposed to a phosphorus screen for 48 h before read. The amount of converted SM was determined by the amount of generated phosphocholine and quantified by pixel densitometry (Lab Works 4.6). After calculating the conversion rate of SM at each SM concentration, the maximal conversion speed (V_{max}) at this protein concentration and K_m were calculated by nonlinear regression (Sigma Plot 11).

Uptake assay for glucose

Radio-labeled substrate uptake experiments were performed as described (Danilchanka *et al.*, 2008a). Cells were grown to OD_{600} 0.8–1.0 in Middlebrook 7H9 medium with detergent (0.02% tyloxapol). Cells were harvested by centrifugation, washed two times in uptake buffer plus detergent (same as that used for growth). The uptake buffer was 15 mM HEPES, 0.9 mM $CaCl_2$, 2.65 mM KCl, 0.5 mM $MgCl_2$, 135 mM NaCl (pH 7.5). Cells were resuspended in uptake buffer and kept on ice until the assay was started. Cells were heated to 37°C immediately before the experiment. ^{14}C-labeled glucose was added to begin the uptake reaction. Cell samples were taken at 1, 2, 3, 4, 8, and 16 minutes, immediately added to killing buffer (0.1 M LiCl in 10% (v/v) phosphate buffered formalin) in a Spin-X tube (Costar) containing a 0.45 μm filter. Samples were centrifuged and washed with killing buffer before the filter was removed and added to scintillation fluid for counting by liquid scintillation.

See supplement for other methods.

Supplementary Material

Refer to Web version on PubMed Central for supplementary material.

Acknowledgments

References

Barry CE 3rd, Boshoff HI, Dartois V, Dick T, Ehrt S, Flynn J, Schnappinger D, Wilkinson RJ, Young D. The spectrum of latent tuberculosis: rethinking the biology and intervention strategies. Nat Rev Microbiol. 2009; 7:845–855. [PubMed: 19855401]

Bernheimer AW, Avigad LS, Kim KS. Staphylococcal sphingomyelinase (beta-hemolysin). Ann N Y Acad Sci. 1974; 236:292–306. [PubMed: 4371058]

Blasband AJ, Marcotte WR Jr, Schnaitman CA. Structure of the *lc* and *nmpC* outer membrane porin protein genes of lambdoid bacteriophage. J Biol Chem. 1986; 261:12723–12732. [PubMed: 3017988]

Boritsch EC, Supply P, Honore N, Seeman T, Stinear TP, Brosch R. A glimpse into the past and predictions for the future: the molecular evolution of the tuberculosis agent. Mol Microbiol. 2014; 93:835–852. [PubMed: 25039682]

Boshoff HI, Myers TG, Copp BR, McNeil MR, Wilson MA, Barry CE 3rd. The transcriptional responses of *Mycobacterium tuberculosis* to inhibitors of metabolism: novel insights into drug mechanisms of action. J Biol Chem. 2004; 279:40174–40184. [PubMed: 15247240]

Brennan PJ, Nikaido H. The envelope of mycobacteria. Annu Rev Biochem. 1995; 64:29–63. [PubMed: 7574484]

Cao Y, Bazemore-Walker CR. Proteomic profiling of the surface-exposed cell envelope proteins of *Caulobacter crescentus*. J Proteomics. 2014; 97:187–194. [PubMed: 23973469]

Clarke CJ, Snook CF, Tani M, Matmati N, Marchesini N, Hannun YA. The extended family of neutral sphingomyelinases. Biochemistry. 2006; 45:11247–11256. [PubMed: 16981685]

Cole C, Barber JD, Barton GJ. The Jpred 3 secondary structure prediction server. Nucleic Acids Res. 2008; 36:W197–201. [PubMed: 18463136]

Danilchanka O, Mailaender C, Niederweis M. Identification of a novel multidrug efflux pump of *Mycobacterium tuberculosis*. Antimicrob Agents Chemother. 2008a; 52:2503–2511. [PubMed: 18458127]

Danilchanka O, Pavlenok M, Niederweis M. Role of porins for uptake of antibiotics by *Mycobacterium smegmatis*. Antimicrob Agents Chemother. 2008b; 52:3127–3134. [PubMed: 18559650]

Danilchanka O, Pires D, Anes E, Niederweis M. The *Mycobacterium tuberculosis* outer membrane channel protein CpnT confers susceptibility to toxic molecules. Antimicrob Agents Chemother. 2015

Danilchanka O, Sun J, Pavlenok M, Maueroder C, Speer A, Siroy A, Marrero J, Trujillo C, Mayhew DL, Doornbos KS, Munoz LE, Herrmann M, Ehrt S, Berens C, Niederweis M. An outer membrane channel protein of *Mycobacterium tuberculosis* with exotoxin activity. Proc Natl Acad Sci U S A. 2014; 111:6750–6755. [PubMed: 24753609]

Doll VM, Ehling-Schulz M, Vogelmann R. Concerted action of sphingomyelinase and non-hemolytic enterotoxin in pathogenic *Bacillus cereus*. PLoS One. 2013; 8:e61404. [PubMed: 23613846]

Domenech P, Reed MB. Rapid and spontaneous loss of phthiocerol dimycocerosate (PDIM) from *Mycobacterium tuberculosis* grown in vitro: implications for virulence studies. Microbiology. 2009; 155:3532–3543. [PubMed: 19661177]

Dubos RJ. The effect of sphingomyelin on the growth of tubercle bacilli. J Exp Med. 1948; 88:73–79. [PubMed: 18871879]

Ehrt S, Rhee K. *Mycobacterium tuberculosis* metabolism and host interaction: mysteries and paradoxes. Curr Top Microbiol Immunol. 2013; 374:163–188. [PubMed: 23242856]

Fabrino DL, Bleck CK, Anes E, Hasilik A, Melo RC, Niederweis M, Griffiths G, Gutierrez MG. Porins facilitate nitric oxide-mediated killing of mycobacteria. Microbes Infect. 2009; 11:868–875. [PubMed: 19460455]

Fajardo DA, Cheung J, Ito C, Sugawara E, Nikaido H, Misra R. Biochemistry and regulation of a novel *Escherichia coli* K-12 porin protein, OmpG, which produces unusually large channels. J Bacteriol. 1998; 180:4452–4459. [PubMed: 9721282]

Finn RD, Bateman A, Clements J, Coggill P, Eberhardt RY, Eddy SR, Heger A, Hetherington K, Holm L, Mistry J, Sonnhammer EL, Tate J, Punta M. Pfam: the protein families database. Nucleic Acids Res. 2014; 42:D222–230. [PubMed: 24288371]

Galagan JE, Sisk P, Stolte C, Weiner B, Koehrsen M, Wymore F, Reddy TB, Zucker JD, Engels R, Gellesch M, Hubble J, Jin H, Larson L, Mao M, Nitzberg M, White J, Zachariah ZK, Sherlock G, Ball CA, Schoolnik GK. TB database 2010: overview and update. Tuberculosis (Edinb). 2010; 90:225–235. [PubMed: 20488753]

Gaus K, Rodriguez M, Ruberu KR, Gelissen I, Sloane TM, Kritharides L, Jessup W. Domain-specific lipid distribution in macrophage plasma membranes. J Lipid Res. 2005; 46:1526–1538. [PubMed: 15863834]

Gonzalez-Zorn B, Dominguez-Bernal G, Suarez M, Ripio MT, Vega Y, Novella S, Vazquez-Boland JA. The smcL gene of *Listeria ivanovii* encodes a sphingomyelinase C that mediates bacterial escape from the phagocytic vacuole. Mol Microbiol. 1999; 33:510–523. [PubMed: 10417642]

Griffin JE, Gawronski JD, Dejesus MA, Ioerger TR, Akerley BJ, Sassetti CM. High-resolution phenotypic profiling defines genes essential for mycobacterial growth and cholesterol catabolism. PLoS Pathog. 2011; 7:e1002251. [PubMed: 21980284]

He X, Chen F, McGovern MM, Schuchman EH. A fluorescence-based, high-throughput sphingomyelin assay for the analysis of Niemann-Pick disease and other disorders of sphingomyelin metabolism. Anal Biochem. 2002; 306:115–123. [PubMed: 12069422]

Hoffmann C, Leis A, Niederweis M, Plitzko JM, Engelhardt H. Disclosure of the mycobacterial outer membrane: cryo-electron tomography and vitreous sections reveal the lipid bilayer structure. Proc Natl Acad Sci U S A. 2008; 105:3963–3967. [PubMed: 18316738]

Huseby M, Shi K, Brown CK, Digre J, Mengistu F, Seo KS, Bohach GA, Schlievert PM, Ohlendorf DH, Earhart CA. Structure and biological activities of beta toxin from *Staphylococcus aureus*. J Bacteriol. 2007; 189:8719–8726. [PubMed: 17873030]

Ingraham LM, Burns CP, Boxer LA, Baehner RL, Haak RA. Fluidity properties and liquid composition of erythrocyte membranes in Chediak-Higashi syndrome. J Cell Biol. 1981; 89:510–516. [PubMed: 7251663]

Johansen KA, Gill RE, Vasil ML. Biochemical and molecular analysis of phospholipase C and phospholipase D activity in mycobacteria. Infect Immun. 1996; 64:3259–3266. [PubMed: 8757862]

Jones CM, Niederweis M. *Mycobacterium tuberculosis* can utilize heme as an iron source. J Bacteriol. 2011; 193:1767–1770. [PubMed: 21296960]

Kartmann B, Stenger S, Niederweis M. Porins in the cell wall of *Mycobacterium tuberculosis*. J Bacteriol. 1999; 181:6543–6546. Authors' correction appeared in J. Bacteriol. 6181, 7650. [PubMed: 10515949]

Keating LA, Wheeler PR, Mansoor H, Inwald JK, Dale J, Hewinson RG, Gordon SV. The pyruvate requirement of some members of the *Mycobacterium tuberculosis* complex is due to an inactive pyruvate kinase: implications for in vivo growth. Mol Microbiol. 2005; 56:163–174. [PubMed: 15773987]

Kennedy GM, Hooley GC, Champion MM, Medie FMba, Champion PA. A novel ESX-1 locus reveals that surface-associated ESX-1 substrates mediate virulence in *Mycobacterium marinum*. J Bacteriol. 2014; 196:1877–1888. [PubMed: 24610712]

Kiefer F, Arnold K, Kunzli M, Bordoli L, Schwede T. The SWISS-MODEL Repository and associated resources. Nucleic Acids Res. 2009; 37:D387–392. [PubMed: 18931379]

King CH, Mundayoor S, Crawford JT, Shinnick TM. Expression of contact-dependent cytolytic activity by *Mycobacterium tuberculosis* and isolation of the genomic locus that encodes the activity. Infect Immun. 1993; 61:2708–2712. [PubMed: 8500911]

Lambert PA. Cellular impermeability and uptake of biocides and antibiotics in Gram-positive bacteria and mycobacteria. J Appl Microbiol. 2002; 92(Suppl):46S–54S. [PubMed: 12000612]

Leyton DL, Rossiter AE, Henderson IR. From self sufficiency to dependence: mechanisms and factors important for autotransporter biogenesis. Nat Rev Microbiol. 2012; 10:213–225. [PubMed: 22337167]

Lichtinger T, Heym B, Maier E, Eichner H, Cole ST, Benz R. Evidence for a small anion-selective channel in the cell wall of *Mycobacterium bovis* BCG besides a wide cation-selective pore. FEBS Lett. 1999; 454:349–355. [PubMed: 10431837]

Lin PL, Rodgers M, Smith L, Bigbee M, Myers A, Bigbee C, Chiosea I, Capuano SV, Fuhrman C, Klein E, Flynn JL. Quantitative comparison of active and latent tuberculosis in the cynomolgus macaque model. Infect Immun. 2009; 77:4631–4642. [PubMed: 19620341]

Lofthouse EK, Wheeler PR, Beste DJ, Khatri BL, Wu H, Mendum TA, Kierzek AM, McFadden J. Systems-based approaches to probing metabolic variation within the Mycobacterium tuberculosis complex. PLoS One. 2013; 8:e75913. [PubMed: 24098743]

Mailaender C, Reiling N, Engelhardt H, Bossmann S, Ehlers S, Niederweis M. The MspA porin promotes growth and increases antibiotic susceptibility of both *Mycobacterium bovis* BCG and *Mycobacterium tuberculosis*. Microbiology. 2004; 150:853–864. [PubMed: 15073295]

Marrero J, Trujillo C, Rhee KY, Ehrt S. Glucose phosphorylation is required for *Mycobacterium tuberculosis* persistence in mice. PLoS Pathog. 2013; 9:e1003116. [PubMed: 23326232]

McDonel JL. *Clostridium perfringens* toxins (type A, B, C, D, E). Pharmacol Ther. 1980; 10:617–655. [PubMed: 6255496]

Neyrolles O, Hernandez-Pando R, Pietri-Rouxel F, Fornes P, Tailleux L, Payan JA, Pivert E, Bordat Y, Aguilar D, Prevost MC, Petit C, Gicquel B. Is adipose tissue a place for *Mycobacterium tuberculosis* persistence? PLoS ONE. 2006; 1:e43. [PubMed: 17183672]

Neyrolles O, Wolschendorf F, Mitra A, Niederweis M. Mycobacteria, metals, and the macrophage. Immunol Rev. 2015; 264:249–263. [PubMed: 25703564]

Niederweis M. Nutrient acquisition by mycobacteria. Microbiology. 2008; 154:679–692. [PubMed: 18310015]

Niederweis M, Danilchanka O, Huff J, Hoffmann C, Engelhardt H. Mycobacterial outer membranes: in search of proteins. Trends Microbiol. 2010; 18:109–116. [PubMed: 20060722]

Niederweis M, Wolschendorf F, Mitra A, Neyrolles O. Mycobacteria, metals and the macrophage. Immunol Rev. 2014 in press.

Nikaido H. Molecular basis of bacterial outer membrane permeability revisited. Microbiol Mol Biol Rev. 2003; 67:593–656. [PubMed: 14665678]

Nikaido H, Jarlier V. Permeability of the mycobacterial cell wall. Res Microbiol. 1991; 142:437–443. [PubMed: 1871430]

Oda M, Hashimoto M, Takahashi M, Ohmae Y, Seike S, Kato R, Fujita A, Tsuge H, Nagahama M, Ochi S, Sasahara T, Hayashi S, Hirai Y, Sakurai J. Role of sphingomyelinase in infectious diseases caused by *Bacillus cereus*. PLoS One. 2012; 7:e38054. [PubMed: 22701599]

Oda M, Takahashi M, Matsuno T, Uoo K, Nagahama M, Sakurai J. Hemolysis induced by *Bacillus cereus* sphingomyelinase. Biochim Biophys Acta. 2010; 1798:1073–1080. [PubMed: 20214877]

Pandey AK, Raman S, Proff R, Joshi S, Kang CM, Rubin EJ, Husson RN, Sassetti CM. Nitrile-inducible gene expression in mycobacteria. Tuberculosis (Edinb). 2009; 89:12–16. [PubMed: 18801704]

Pandey AK, Sassetti CM. Mycobacterial persistence requires the utilization of host cholesterol. Proc Natl Acad Sci USA. 2008; 105:4376–4380. [PubMed: 18334639]

Parker SK, Barkley RM, Rino JG, Vasil ML. Mycobacterium tuberculosis Rv3802c encodes a phospholipase/thioesterase and is inhibited by the antimycobacterial agent tetrahydrolipstatin. PLoS One. 2009; 4:e4281. [PubMed: 19169353]

Portevin D, De Sousa-D'Auria C, Houssin C, Grimaldi C, Chami M, Daffe M, Guilhot C. A polyketide synthase catalyzes the last condensation step of mycolic acid biosynthesis in mycobacteria and related organisms. Proc Natl Acad Sci USA. 2004; 101:314–319. [PubMed: 14695899]

Prados-Rosales R, Baena A, Martinez LR, Luque-Garcia J, Kalscheuer R, Veeraraghavan U, Camara C, Nosanchuk JD, Besra GS, Chen B, Jimenez J, Glatman-Freedman A, Jacobs WR Jr, Porcelli SA, Casadevall A. Mycobacteria release active membrane vesicles that modulate immune responses in a TLR2-dependent manner in mice. J Clin Invest. 2011; 121:1471–1483. [PubMed: 21364279]

Puckett S, Trujillo C, Eoh H, Marrero J, Spencer J, Jackson M, Schnappinger D, Rhee K, Ehrt S. Inactivation of fructose-1,6-bisphosphate aldolase prevents optimal co-catabolism of glycolytic and gluconeogenic carbon substrates in *Mycobacterium tuberculosis*. PLoS Pathog. 2014; 10:e1004144. [PubMed: 24851864]

Ratledge C. Iron, mycobacteria and tuberculosis. Tuberculosis. 2004; 84:110–130. [PubMed: 14670352]

Raynaud C, Guilhot C, Rauzier J, Bordat Y, Pelicic V, Manganelli R, Smith I, Gicquel B, Jackson M. Phospholipases C are involved in the virulence of *Mycobacterium tuberculosis*. Mol Microbiol. 2002; 45:203–217. [PubMed: 12100560]

Rohde K, Yates RM, Purdy GE, Russell DG. *Mycobacterium tuberculosis* and the environment within the phagosome. Immunol Rev. 2007; 219:37–54. [PubMed: 17850480]

Russell DG. *Mycobacterium tuberculosis* and the intimate discourse of a chronic infection. Immunol Rev. 2011; 240:252–268. [PubMed: 21349098]

Russell DG, Cardona PJ, Kim MJ, Allain S, Altare F. Foamy macrophages and the progression of the human tuberculosis granuloma. Nat Immunol. 2009; 10:943–948. [PubMed: 19692995]

Russell DG, VanderVen BC, Lee W, Abramovitch RB, Kim MJ, Homolka S, Niemann S, Rohde KH. *Mycobacterium tuberculosis* wears what it eats. Cell Host Microbe. 2010; 8:68–76. [PubMed: 20638643]

Sassetti CM, Rubin EJ. Genetic requirements for mycobacterial survival during infection. Proc Natl Acad Sci USA. 2003; 100:12989–12994. [PubMed: 14569030]

Schnappinger D, Ehrt S, Voskuil MI, Liu Y, Mangan JA, Monahan IM, Dolganov G, Efron B, Butcher PD, Nathan C, Schoolnik GK. Transcriptional adaptation of *Mycobacterium tuberculosis* within macrophages: Insights into the phagosomal environment. J Exp Med. 2003; 198:693–704. [PubMed: 12953091]

Simeone R, Bobard A, Lippmann J, Bitter W, Majlessi L, Brosch R, Enninga J. Phagosomal rupture by *Mycobacterium tuberculosis* results in toxicity and host cell death. PLoS Pathog. 2012; 8:e1002507. [PubMed: 22319448]

Skaar EP. The battle for iron between bacterial pathogens and their vertebrate hosts. PLoS Pathog. 2010; 6:e1000949. [PubMed: 20711357]

Smith J, Manoranjan J, Pan M, Bohsali A, Xu J, Liu J, McDonald KL, Szyk A, LaRonde-LeBlanc N, Gao LY. Evidence for pore formation in host cell membranes by ESX-1-secreted ESAT-6 and its role in *Mycobacterium marinum* escape from the vacuole. Infect Immun. 2008; 76:5478–5487. [PubMed: 18852239]

Song H, Niederweis M. Uptake of sulfate but not phosphate by *Mycobacterium tuberculosis* is slower than that for *Mycobacterium smegmatis*. J Bacteriol. 2012; 194:956–964. [PubMed: 22194452]

Song H, Sandie R, Wang Y, Andrade-Navarro MA, Niederweis M. Identification of outer membrane proteins of *Mycobacterium tuberculosis*. Tuberculosis. 2008; 88:526–544. [PubMed: 18439872]

Speer A, Rowland JL, Haeili M, Niederweis M, Wolschendorf F. Porins increase copper susceptibility of *Mycobacterium tuberculosis*. J Bacteriol. 2013a; 195:5133–5140. [PubMed: 24013632]

Speer A, Rowland JL, Niederweis M. *Mycobacterium tuberculosis* is resistant to streptolydigin. Tuberculosis (Edinb). 2013b; 93:401–404. [PubMed: 23591156]

Stahl C, Kubetzko S, Kaps I, Seeber S, Engelhardt H, Niederweis M. MspA provides the main hydrophilic pathway through the cell wall of *Mycobacterium smegmatis*. Mol Microbiol. 2001; 40:451–464. Authors' correction appeared in Mol. Microbiol. 457, 1509. [PubMed: 11309127]

Steinbrecher UP, Gomez-Munoz A, Duronio V. Acid sphingomyelinase in macrophage apoptosis. Curr Opin Lipidol. 2004; 15:531–537. [PubMed: 15361788]

Stephan J, Bender J, Wolschendorf F, Hoffmann C, Roth E, Mailänder C, Engelhardt H, Niederweis M. The growth rate of *Mycobacterium smegmatis* depends on sufficient porin-mediated influx of nutrients. Mol Microbiol. 2005; 58:714–730. [PubMed: 16238622]

Stephan J, Mailaender C, Etienne G, Daffe M, Niederweis M. Multidrug resistance of a porin deletion mutant of *Mycobacterium smegmatis*. Antimicrob Agents Chemother. 2004; 48:4163–4170. [PubMed: 15504836]

Van der Geize R, Yam K, Heuser T, Wilbrink MH, Hara H, Anderton MC, Sim E, Dijkhuizen L, Davies JE, Mohn WW, Eltis LD. A gene cluster encoding cholesterol catabolism in a soil actinomycete provides insight into *Mycobacterium tuberculosis* survival in macrophages. Proc Natl Acad Sci USA. 2007; 104:1947–1952. [PubMed: 17264217]

van der Wel N, Hava D, Houben D, Fluitsma D, van Zon M, Pierson J, Brenner M, Peters PJ. *M. tuberculosis* and *M. leprae* translocate from the phagolysosome to the cytosol in myeloid cells. Cell. 2007; 129:1287–1298. [PubMed: 17604718]

Vargas-Villarreal J, Mata-Cardenas BD, Deslauriers M, Quinn FD, Castro-Garza J, Martinez-Rodrlguez HG, Said-Fernandez S. Identification of acidic, alkaline, and neutral sphingomyelinase activities in *Mycobacterium tuberculosis*. Med Sci Monit. 2003; 9:BR225–230. [PubMed: 12824945]

Voskuil MI, Visconti KC, Schoolnik GK. *Mycobacterium tuberculosis* gene expression during adaptation to stationary phase and low-oxygen dormancy. Tuberculosis. 2004; 84:218–227. [PubMed: 15207491]

Voss BJ, Gaddy JA, McDonald WH, Cover TL. Analysis of surface-exposed outer membrane proteins in Helicobacter pylori. J Bacteriol. 2014

Wang L, Slayden RA, Barry CE 3rd, Liu J. Cell wall structure of a mutant of *Mycobacterium smegmatis* defective in the biosynthesis of mycolic acids. J Biol Chem. 2000; 275:7224–7229. [PubMed: 10702292]

Watanabe S, Zimmermann M, Goodwin MB, Sauer U, Barry CE 3rd, Boshoff HI. Fumarate reductase activity maintains an energized membrane in anaerobic *Mycobacterium tuberculosis*. PLoS Pathog. 2011; 7:e1002287. [PubMed: 21998585]

Wolf AJ, Linas B, Trevejo-Nunez GJ, Kincaid E, Tamura T, Takatsu K, Ernst JD. *Mycobacterium tuberculosis* infects dendritic cells with high frequency and impairs their function in vivo. J Immunol. 2007; 179:2509–2519. [PubMed: 17675513]

Wolschendorf F, Mahfoud M, Niederweis M. Porins are required for uptake of phosphates by *Mycobacterium smegmatis*. J Bacteriol. 2007; 189:2435–2442. [PubMed: 17209034]

Wong D, Bach H, Sun J, Hmama Z, Av-Gay Y. *Mycobacterium tuberculosis* protein tyrosine phosphatase (PtpA) excludes host vacuolar-H+-ATPase to inhibit phagosome acidification. Proc Natl Acad Sci U S A. 2011; 108:19371–19376. [PubMed: 22087003]

Xu G, Jia H, Li Y, Liu X, Li M, Wang Y. Hemolytic phospholipase Rv0183 of Mycobacterium tuberculosis induces inflammatory response and apoptosis in alveolar macrophage RAW264.7 cells. Can J Microbiol. 2010; 56:916–924. [PubMed: 21076482]

Zhang YJ, Ioerger TR, Huttenhower C, Long JE, Sassetti CM, Sacchettini JC, Rubin EJ. Global assessment of genomic regions required for growth in *Mycobacterium tuberculosis*. PLoS Pathog. 2012; 8:e1002946. [PubMed: 23028335]
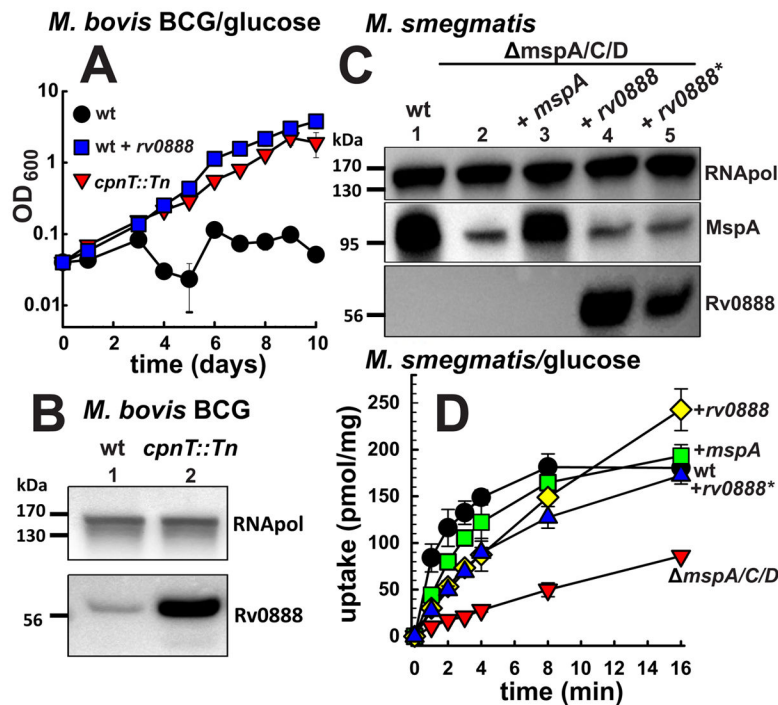
Fig. 1. Rv0888 mediates glucose uptake in mycobacteria

(**A**) Growth of *M. bovis* BCG strains ML383 (wt, black), ML386 (*cpnT::Tn*, red) and wt expressing *rv0888* (pML2102) (blue) in HdB medium supplemented with 1% glucose. OD_{600} of ML383 and wt expressing *rv0888* is significantly higher (p-value < 0.001) compared to the *cpnT::Tn* mutant in every time point starting day 5. The data was analysed by one-way ANOVA followed by a Tukey test. (**B**) Western blot analysis of *M. bovis* BCG wt and the *cpnT::Tn* mutant. Rv0888 was detected with an Rv0888-specific antiserum. *M. bovis* BCG RNA polymerase (RNApol) was detected on the same blot with monoclonal antibodies. Lanes: 1, ML383 (wt); 2, ML386 (*cpnT::Tn*). (**C**) Western blot analysis of *M. smegmatis* SMR5 (wt) and porin deletion strain ML16 (*mspA, mspC, mspD*) expressing *mspA*, *rv0888* or the enzymatic mutant *rv0888**. Rv0888 was detected with an Rv0888-specific antiserum. *M. smegmatis* RNA polymerase (RNApol) and MspA were detected on the same blot. Lanes: 1, SMR5/pMS2kan (wt, empty vector); 2, ML16/pMS2kan (empty vector); 3, ML16/pML632 (+*mspA*); 4, ML16/pML2118 (+*rv0888*); 5, ML16/pML3108 (+*rv0888**). (**D**) Accumulation of ^{14}C-glucose by *M. smegmatis* strains SMR5/pMS2kan (wt, empty vector, black), ML16/pMS2kan (empty vector, red), ML16/pML632 (+*mspA*, green), ML16/pML2118 (+*rv0888*, yellow) and ML16/pML3108 (+*rv0888**, blue) was measured. The uptake rate is expressed as pmol of glucose per milligram of dried cells. Mean values of biological triplicates are shown with standard deviations. The uptake of glucose in all tested strains is significantly higher (p-value < 0.001) compared to ML16 (pMS2kan) after 1 min. The p-values were calculated by one-way ANOVA followed by a Tukey test.
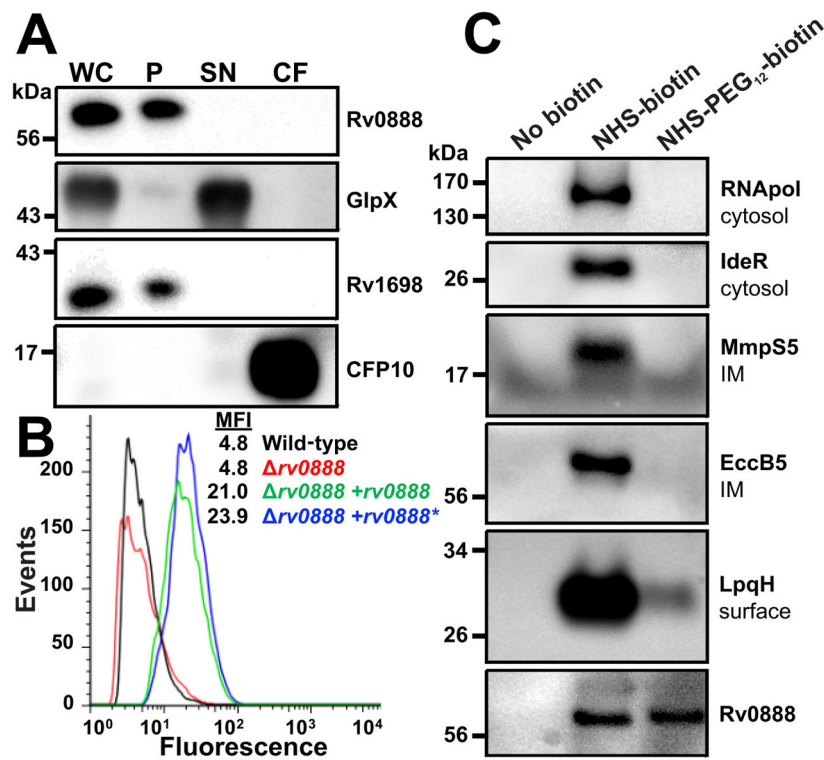
Fig. 2. Rv0888 is an outer membrane protein of *M. tuberculosis*

(**A**) Subcellular localization of Rv0888. Mtb mc^{2}6206 (wt) cells were lysed (WC) and water soluble (SN) and insoluble proteins (P) were separated by centrifugation. The culture supernatant was concentrated 500-fold (CF). Proteins from each fraction were analyzed by Western blot. Rv0888 was detected with an Rv0888-specific antiserum. GlpX, Rv1698 and CFP10 served as marker proteins for soluble proteins (SN), membrane associated proteins (P) and secreted proteins (CF), respectively. (**B**) Surface accessibility of Rv0888. Cells of Mtb ML1528 (H37Rv L5::pCV125), ML1566 (*rv0888::loxP*), ML923 (*rv0888::loxP, L5::rv0888*) and ML925 (*rv0888::loxP, L5::rv0888**) were incubated with a monoclonal anti-Rv0888 antibody (10E2.7) followed by detection with anti-mouse FITC-labeled antibody. The fluorescence of surface-stained Mtb cells was measured by flow cytometry and is displayed as histograms (MFI, mean fluorescence intensity). The MFI of strains ML923 and ML925 is significant higher (p-value < 0.05, Chi-Squared T(X) > 500) when compared to ML1528 or ML1566. (**C**) Whole cells of Mtb mc^{2}6206 (wt) were biotinylated. Cells were lysed and biotinylated proteins were purified using a Strep-Avidin column. An untreated sample served as a control for unspecific binding. After elution samples were analyzed by Western blot. Proteins of known subcellular localization served as control for cytosolic proteins (RNApol, IdeR), inner membrane associated proteins (MmpS5, EccB5) and surface assessable proteins (LpqH).
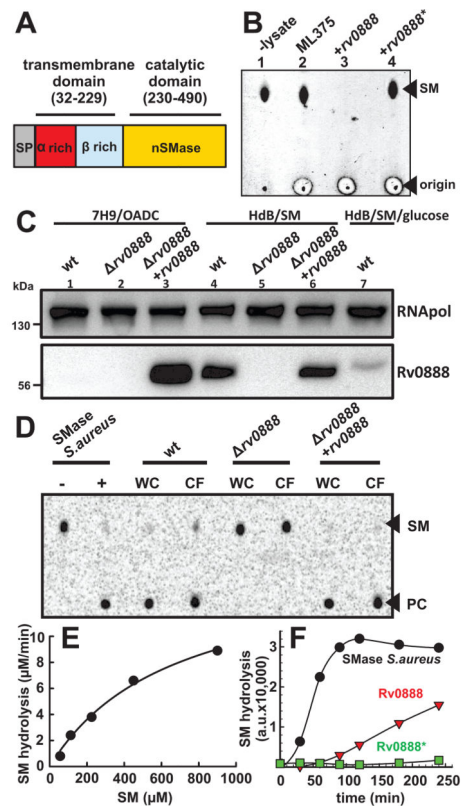
Fig. 3. Rv0888 has a C-terminal sphingomyelinase domain

(A) Predicted domain organization of Rv0888. Rv0888 encodes for a Sec-signal sequence which is cleaved after residue 31. The secondary structure of Rv0888 between residues 31–229 is predicted to have a high content of hydrophobic β-sheets. The C-terminus (residue 230–490) contains conserved residues found in neutral sphingomyelinases. **(B)** Sphingomyelinase activity of *M. smegmatis* strains using TLC analysis. Whole cell lysates of *M. smegmatis* porin mutant ML375 (mspA, mspC, mspD groEL-5ʹ) and ML375 expressing *rv0888* (pML2100) or the enzymatic mutant *rv0888** (pML3109) were incubated with 100 ng sphingomyelin (SM). After 2 h of incubation amounts corresponding to 5 ng SM were transferred onto a TLC plate (origin) and resolved using chloroform/methanol/ water (65:20:1, vol/vol). Phospholipids were visualized by the Dittmer-Lester reagent. Lanes: 1, SM in reaction buffer; 2, ML375; 3, ML375/pML2100 (+*rv0888*); 4, ML375/ pML3109 (+*rv0888**). PC; phosphocholine. **(C)** Western blot analysis of Mtb *rv0888* deletion strain. Mtb strains H37Rv (wt), rv0888 and rv0888 expressing *rv0888* were analyzed by Western blot after growing in 7H9/OADC or in HdB supplemented with 0.75 mM sphingomyelin (HdB/SM) or 0.75 mM sphingomyelin and 0.2% glucose (HdB/SM/ glucose). Rv0888 was detected with monoclonal anti-Rv0888 antibody (10E2.7), Mtb RNA polymerase (RNApol) served as a loading control. The signals were quantified by pixel-densitometry. Lanes: 1, ML1528 (H37Rv L5::pCV125; wt); 2, ML1566 (*rv0888::loxP*); 3, ML923 (*rv0888::loxP, L5::rv0888*); 4, ML1528; 5, ML1566; 6, ML923; 7, ML1528. **(D)** Mtb whole cell lysates (WC) and concentrated culture filtrates of the corresponding strain were incubated with 7 μM of ^{14}C- SM for 48 h at 37°C before analysis by thin layer chromatography (TLC). Sphingomyelinase of *S. aureus* served as a positive control. PC:

phosphocholine. **(E)** Rv0888 protein purified from *E. coli* (14.6 pM) was incubated with 0.18, 0.35, 1.8, 3.5, 18 and 35 μM ^{14}C-sphingomyelin (SM). The reaction products were separated by TLC and the amount of cleaved phosphocholine (PC) was determined by densitometry. The SM hydrolysis rates were blotted against the substrate concentration. The Michaelis-Menten parameters v_{max} and K_m were calculated by non-linear regression to be 15.72 μM/min and 671 μM, respectively. A detailed data analysis is shown in Fig. S6. **(F)** Enzymatic sphingomyelinase assay using purified proteins. 1.5 μg of purified Rv0888 and Rv0888* proteins were analyzed using the fluorometric Amplex Red sphingomyelinase assay. SM hydrolysis is indicated by fluorescence in arbitrary units (a.u.). The activity of Rv0888 protein was calculated using the slopes of the fastest SM hydrolysis by Rv0888 and the *S. aureus* sphingomyelinase (0.04 units/mL).
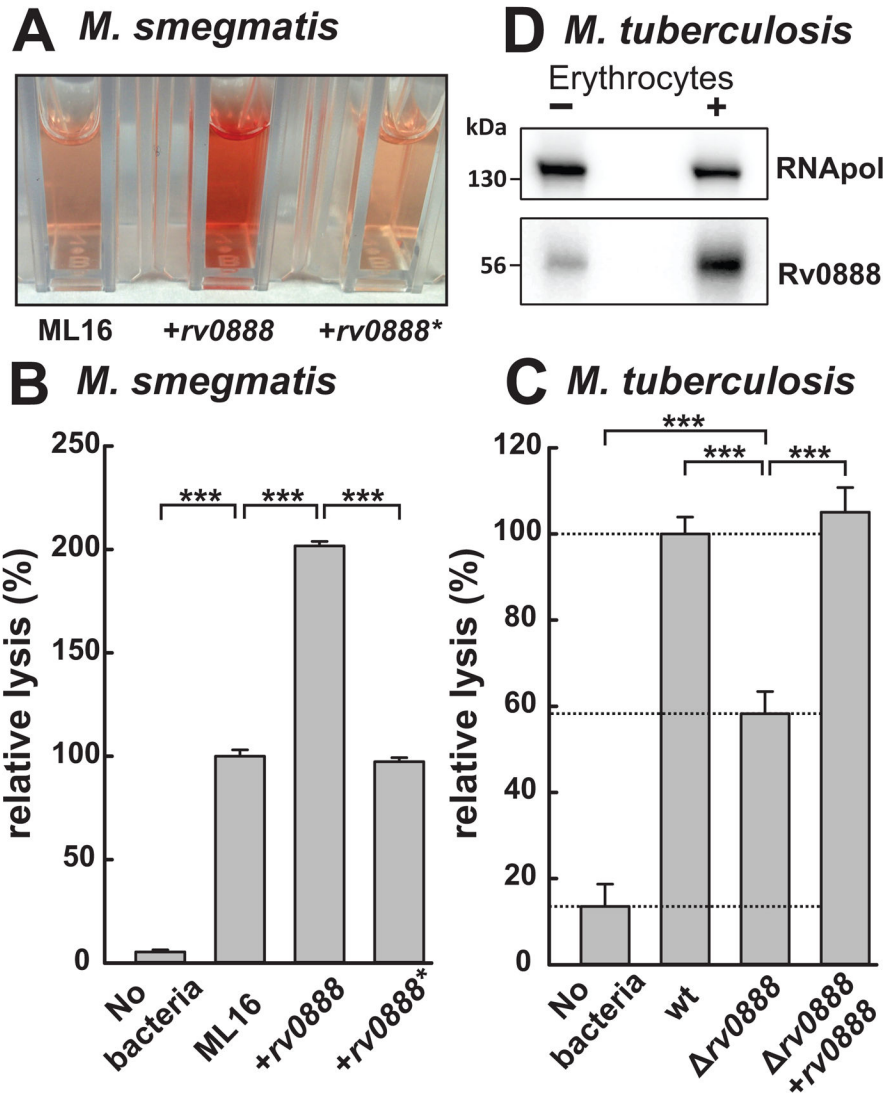
Fig. 4. The sphingomyelinase Rv0888 mediates contact-dependent hemolysis

Bacterial cells of *M. smegmatis* and Mtb were incubated with human blood (MOI 500) at 37°C for 18 h and 24 h, respectively. The intact erythrocytes and bacterial cells were removed by centrifugation and the supernatants containing the released hemoglobin were transferred into cuvettes and quantified by determining the absorbance at 540 nm. A bacteria free sample served as a control for autolysis of erythrocytes. **(A)** Supernatant of erythrocytes incubated with the *M. smegmatis* porin mutant ML16 (mspA, mspC, mspD), ML16 expressing *rv0888* (pML2118) or the enzymatic mutant *rv0888** (pML3108) was quantified spectroscopically **(B). (C)** Hemolysis caused by Mtb ML1528 (H37Rv L5::pCV125; wt), ML1566 (*rv0888::loxP*) and ML923 (*rv0888::loxP, L5::rv0888*). Wt Mtb and *M. smegmatis* cells lysed 50% of all erythrocytes as determined by complete lysis with 0.5% SDS. Mean values of biological triplicates are shown with standard deviations. Lysis is expressed in relative values normalized to wt Mtb and wt *M. smegmatis* cells as 100%. The P values were calculated by a one-way ANOVA in combination with a Tukey test and are denoted as

follows: * ($p < 0.05$), ** ($p < 0.01$), *** ($p < 0.001$). **(D)** Western blot analysis of Mtb wt cells in contact with erythrocytes for 24 h. Rv0888 was detected with monoclonal anti-Rv0888 antibody (10E2.7), Mtb RNA polymerase (RNApol) served as a loading control.
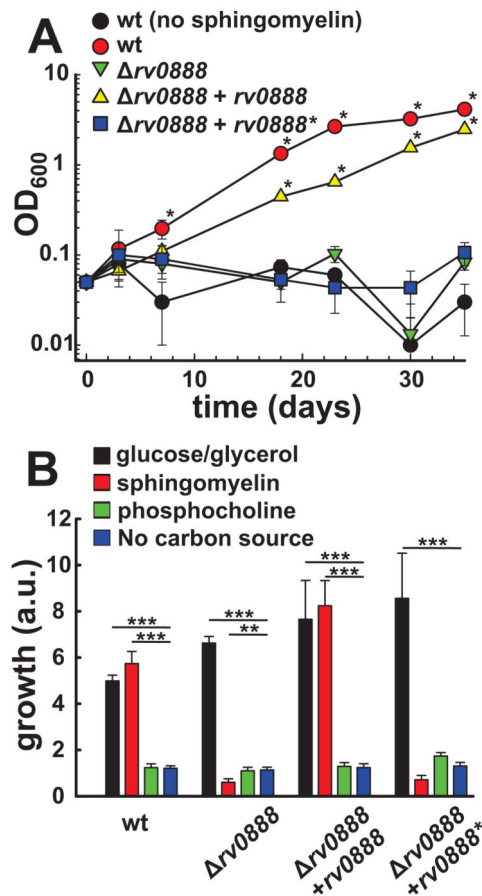
Fig. 5. Sphingomyelinase activity of Rv0888 is required for growth of *Mtb* on sphingomyelin
(A/B) Growth of Mtb strains ML1528 (H37Rv L5::pCV125; wt; red), ML1566
(*rv0888::loxP*, green), ML923 (*rv0888::loxP, L5::rv0888*, yellow) and ML925
(*rv0888::loxP, L5::rv0888**, blue) in HdB medium with different carbon sources. **(A)** Mtb
strains were grown in HdB with 0.75 mM sphingomyelin as sole carbon source. As control
served Mtb ML1528 grown in HdB medium without sphingomyelin to ensure the absence of
other carbon source (black). Growth was monitored by changes in optical density (OD_{600}).
Average values of technical triplicates are shown with standard deviations. An OD_{600} of
ML1528 and ML923 that is significantly higher compared to ML1528 (no SM), ML1566
and ML925 is indicated with an asterik (p-value < 0.001). **(B)** Mtb strains were grown in
HdB medium with 0.38 mM sphingomyelin, 0.38 mM phosphocholine or 15 mM glucose
and 15 mM glycerol as carbon sources in a 96-well plate for two weeks. Growth of bacteria
was determined by fluorescence after addition of the dye resazurin and is indicated by
arbitrary units (a.u.). Average values of technical triplicates are shown with standard
deviations. Values marked with asterisks are significantly different compared to the carbon
source free culture. The data was logarithmically transformed to achieve normal distribution
and a one-way ANOVA in combination with a Tukey test was performed. The p values are *
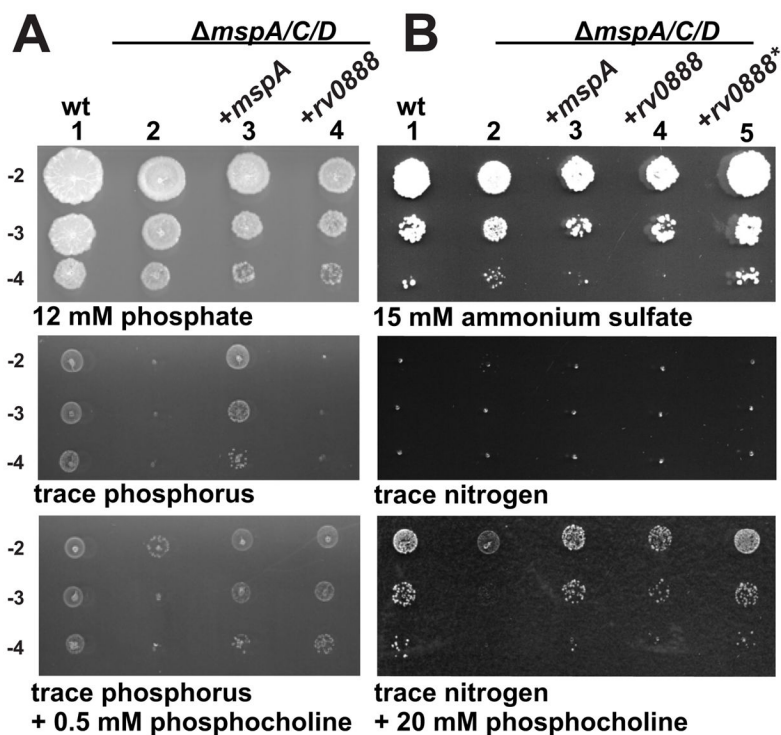($p < 0.05$); ** ($p < 0.01$); *** ($p < 0.001$).

Fig. 6. Rv0888 enables utilization of sphingomyelin cleavage products as nutrient sources
Phosphocholine utilization of *M. smegmatis* SMR5 (wt), the *M. smegmatis* porin mutant ML16 (ΔmspA, ΔmspC, ΔmspD) and ML16 expressing *mspA, rv0888* or *rv0888**. Ten-fold serial diluted cultures were dropped on **(A) low-phosphate** HdB/kan plates with regular amounts of phosphate (12 mM), no phosphate (trace phosphorus) and HdB plates with trace amounts of phosphorus supplemented with 0.5 mM phosphocholine. **(B)** Diluted cells were transferred on **low-nitrogen** HdB/kan plates with regular amounts of ammonium sulfate (15 mM), no ammonium sulfate (trace nitrogen) and HdB plates with trace amounts of nitrogen supplemented with 20 mM phosphocholine. The concentration of phosphocholine in these experiments was determined empirically. Lanes: 1, SMR5/pMS2kan (wt, empty vector); 2, ML16/pMS2kan (empty vector); 3, ML16/pML632 (+*mspA*); 4, ML16/pML2118 (+*rv0888*); 5, ML16/pML3108 (+*rv0888**).
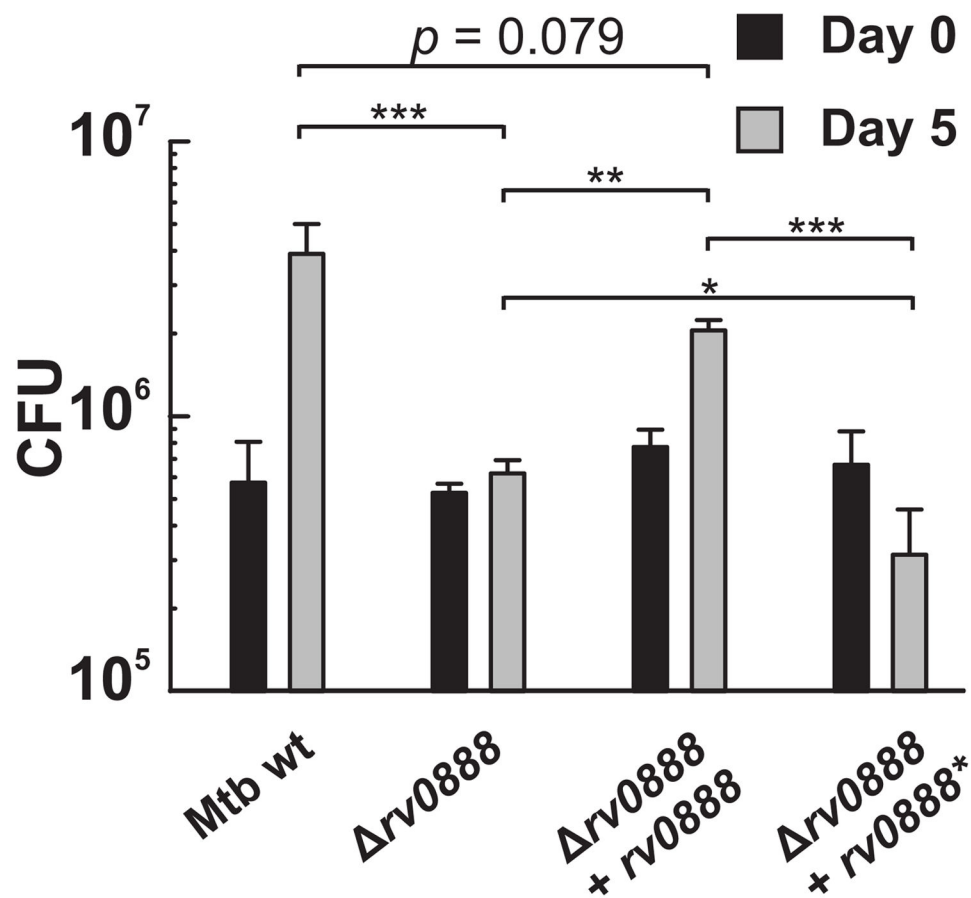
Fig. 7. Expression of *rv0888* enhances intracellular replication of *M. tuberculosis* in macrophages
Differentiated THP-1 macrophages were infected with Mtb ML1528 (H37Rv L5::pCV125; wt), ML1566 (*rv0888::loxP*), ML923 (*rv0888::loxP, L5::rv0888*) and ML925 (*rv0888::loxP, L5::rv0888**) at an MOI of 1. Bacterial strains were grown in HdB medium supplemented with 0.75 mM sphingomyelin and 0.2% glucose to logarithmic phase before infection. Macrophages were lysed after 4 h and 5 days post-infection and the number of viable bacteria was counted as colony forming units (CFU) on agar plates. Mean values of biological triplicates are shown with standard deviations. The data was logarithmically transformed to achieve normal distribution and a one-way ANOVA in combination with a Tukey test was performed. The p values are * ($p < 0.05$); ** ($p < 0.01$); *** ($p < 0.001$).
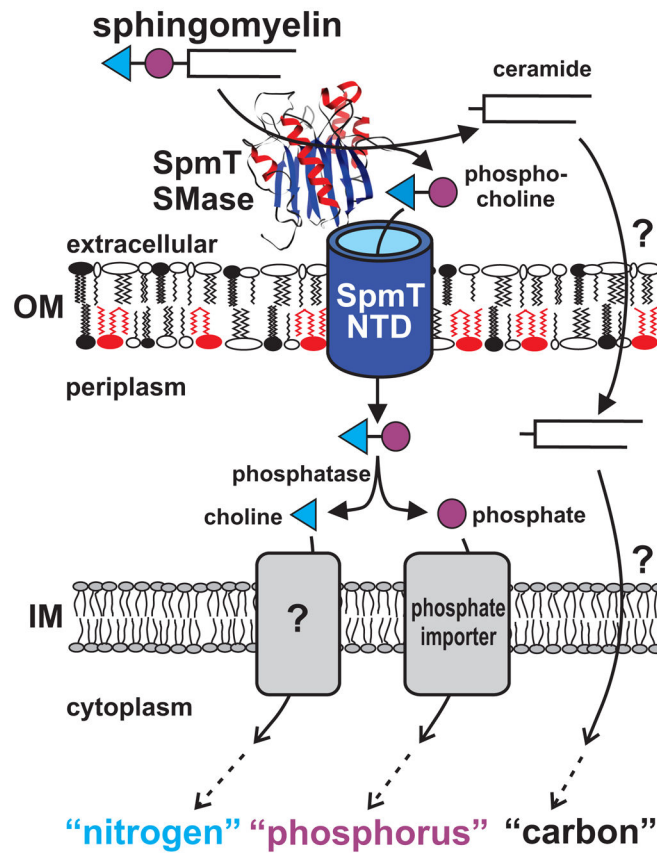
Fig. 8. Role of SpmT (Rv0888) in utilization of sphingomyelin as a versatile nutrient source by *M. tuberculosis*

SpmT (Rv0888) is an outer membrane protein of Mtb and consists of two domains. The C-terminal domain is a cell-surface sphingomyelinases which catalyzes the hydrolysis of SM into phosphocholine and ceramide. The N-terminal domain inserts into the outer membrane (OM) and may facilitate uptake of phosphocholine. Ceramide is utilized by Mtb as a carbon source after uptake by an unknown mechanism. The phosphate group of phosphocholine might be cleaved off by the alkaline phosphatase in the periplasm and taken up by an inner membrane (IM) phosphate transporter. It is unclear how choline is taken up and utilized as a nitrogen source. This model visualizes how the sphingomyelinase SpmT enables Mtb to utilize sphingomyelin as a nutrient source for carbon, nitrogen and phosphorus.